WWW.OEAW.AC.AT

ÖAW ÖSTERREICHISCHE AKADEMIE DER WISSENSCHAFTEN

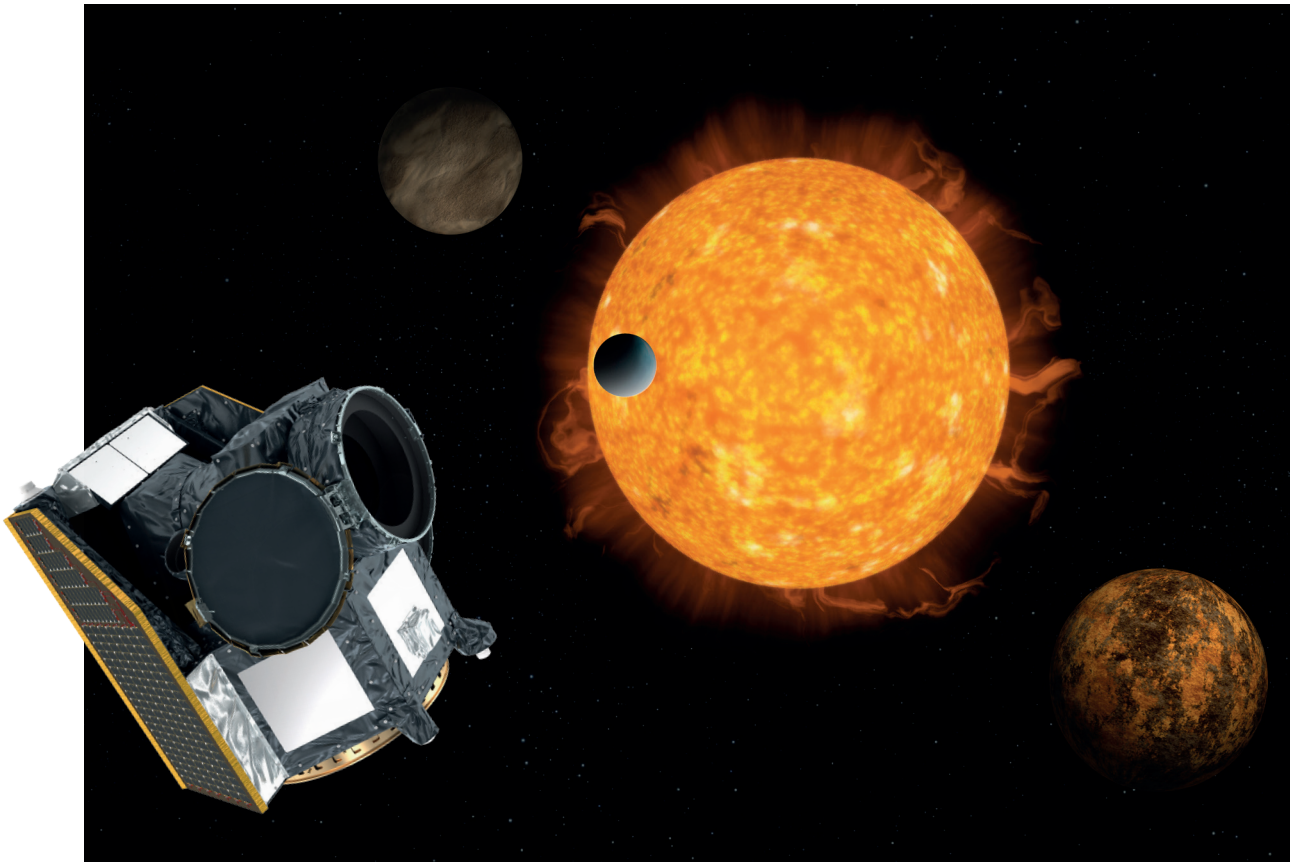

ANNUAL REPORT 2019

IWF INSTITUT FÜR WELTRAUMFORSCHUNG

WWW.IWF.OEAW.AC.AT

ÖAW ÖSTERREICHISCHE AKADEMIE DER WISSENSCHAFTEN

IWF INSTITUT FÜR WELTRAUMFORSCHUNG

COVER IMAGE

Artist impression of *CHEOPS*, the *CHaracterising ExOPlanet Satellite*, with an exoplanet system in the background (© ESA/ATG medialab).

TABLE OF CONTENTS

INTRODUCTION

The Space Research Institute (Institut für Weltraumforschung, IWF) in Graz focuses on the physics of space plasmas and (exo-)planets. With about 100 staff members from 20 nations it is one of the largest institutes of the Austrian Academy of Sciences (Österreichische Akademie der Wissenschaften, ÖAW).

IWF develops and builds space-qualified instruments and analyzes and interprets the data returned by them. Its core engineering expertise is in building magnetometers and on-board computers, as well as in satellite laser ranging, which is performed at a station operated by IWF at the Lustbühel Observatory. In terms of science, the institute concentrates on dynamical processes in space plasma physics and on the upper atmospheres of planets and exoplanets.

IWF cooperates closely with space agencies all over the world and with numerous other national and international research institutions. A particularly intense cooperation exists with the European Space Agency (ESA).

The institute is currently involved in twenty-one active and future international space missions; among these:

- ESA's *Cluster* mission, launched in 2000, still provides unique data to better understand space plasmas.
- *MMS*, launched in 2015, uses four identically equipped spacecraft to explore the acceleration processes that govern the dynamics of the Earth's magnetosphere.
- The first *China Seismo-Electromagnetic Satellite (CSES-1)* was launched in 2018 to study the Earth's ionosphere. CSES-2 will follow in 2022.
- *BepiColombo*, launched in 2018, is on its way to Mercury. It will investigate the planet, using two orbiters, one specialized in magnetospheric studies and one in remote sensing.
- The Korean satellite *GEO-KOMPSAT-2A (GK-2A)* was launched in 2018 to conduct space weather investigations.
- ESA's first small (S-class) mission *CHEOPS (CHaracterizing ExOPlanets Satellite)* was successfully launched on 18 December 2019. The satellite flies at an altitude of about 700 km and observes roughly 500 bright stars, to characterize their planets.

CHEOPS lifts off from Europe's spaceport in Kourou, French Guiana (© ESA).

- Along an innovative trajectory, *Solar Orbiter* (launched in early 2020) is to study solar and heliospheric phenomena.
- ESA's *JUpiter ICy moons Explorer (JUICE)* will investigate Jupiter and three of its largest moons, Ganymede, Callisto, and Europa. It is planned for launch in 2022.
- *SMILE*, scheduled for launch in 2023, is designed to study the interaction between the solar wind and Earth's magnetosphere.
- ESA's third medium (M-class) science mission *PLATO* is a space-based observatory to search for planets orbiting alien stars. It is planned for launch by 2026.

HIGHLIGHTS IN 2019

- A "Nature Communications" study presented the first evidence of standing waves on the dayside magnetopause using the five *THEMIS* satellites.
- Three-dimensional numerical simulations provided new insights into energy conversion processes in space. How space plasmas can be heated was reported in "Physical Review Letters".
- Astronomers identified three new planetary systems for a total of six planets. This discovery may lead to the characterization of exoplanet geology. The three studies were published in "Nature Astronomy".
- The successful launch of *CHEOPS* marked the highlight in the last month of 2019.

THE YEAR 2019 IN NUMBERS

Members of the institute published 142 papers in refereed international journals, of which 42 were first author publications. During the same period, articles with authors from the institute were cited 5705 times in the international literature. In addition, 70 talks and 55 posters were presented at international conferences by IWF members. Last but not least, institute members were involved in the organization of six international meetings or workshops.

IWF STRUCTURE AND FUNDING

IWF is structured into six research groups (see figure). Wolfgang Baumjohann serves as Director, Werner Magnes as Deputy Director.

Most financial support is provided by ÖAW. Significant support is also given by other national institutions, in particular the Austrian Research Promotion Agency (Österreichische Forschungsförderungsgesellschaft, FFG) and the Austrian Science Fund (Fonds zur Förderung der wissenschaftlichen Forschung, FWF). Furthermore, European institutions like ESA and the European Union contribute substantially.

IWF research fields and group leaders.

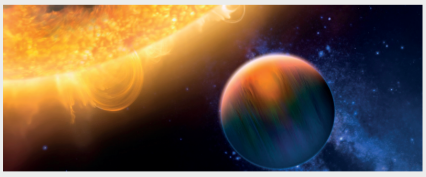

EXOPLANETS

Lead: Luca Fossati

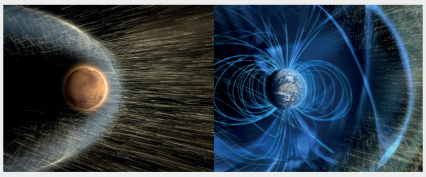

PLANETARY ATMOSPHERES

Lead: Helmut Lammer

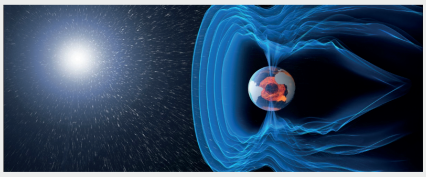

SPACE PLASMA PHYSICS

Lead: Rumi Nakamura

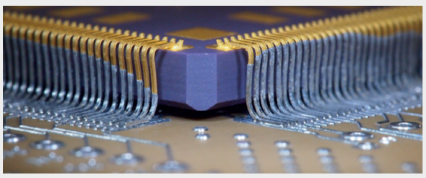

ON-BOARD COMPUTERS

Lead: Manfred Steller

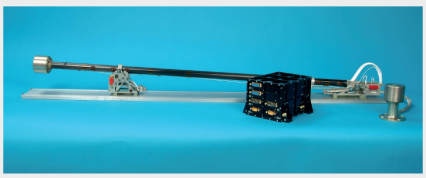

SPACE MAGNETOMETERS

Lead: Werner Magnes

SATELLITE LASER RANGING

Lead: Georg Kirchner

NEAR-EARTH SPACE

Near-Earth space is a most suitable place to study fundamental space plasma processes through recent advancements in the in-situ measurements of charged particles together with electric and magnetic fields at high cadence. IWF has been participating in the hardware activities of numerous space missions in the Earth's magnetosphere, now under operation as well as in the planning phase. Data taken from these missions have been extensively analyzed at IWF by applying different analysis methods to the data and by theoretical modeling to compare with the observations. The obtained results contribute to enhancing the knowledge about space plasma processes applicable in other plasma environments within our solar system and beyond.

CLUSTER

The *Cluster* spacecraft have been providing data since 2001 for studying small-scale structures of the magnetosphere and its environment as the first four-satellite mission in space. The mission is currently planned to be extended to December 2020. IWF is PI/Co-Investigator on five instruments and has contributed to data archiving activities at the *Cluster Science Archives (CSA)* in addition to science data analysis.

MMS

NASA's *MMS (Magnetospheric Multi-Scale)* mission, launched in 2015, explores the dynamics of the Earth's magnetosphere and its underlying energy transfer processes. Four identically equipped spacecraft carry out measurements in the Earth's magnetosphere with high temporal and spatial resolution. *MMS* investigates the small-scale basic plasma processes, which transport, accelerate and energize plasmas in thin boundary and current layers. After successful completion of the science phase and the first extension phase, the second extension phase is being proposed for further five years where observations by a new constellation of the spacecraft is planned.

IWF has taken the lead for the spacecraft potential control *(ASPOC)* and is participating in the electron beam instrument *(EDI)* and the digital fluxgate magnetometer *(DFG)*. In addition to the operation of these instruments and scientific data analysis, IWF is contributing to inflight calibration activities.

THEMIS/ARTEMIS

NASA's *THEMIS* mission *(Time History of Events and Macroscale Interactions during Substorms)*, launched in 2007, consists of five identical satellites flying through different regions of the magnetosphere. In autumn 2010 the two outer spacecraft became *ARTEMIS* and are orbiting the Moon, while the other three *THEMIS* spacecraft remained in their orbit. As Co-Investigator of the magnetometer, IWF is participating in processing and analyzing data.

SMILE

The *Solar wind Magnetosphere Ionosphere Link Explorer (SMILE)* is a joint mission between ESA and the Chinese Academy of Sciences (CAS), scheduled for launch in 2023. It aims to build a more complete understanding of the Sun-Earth connection by measuring the solar wind and its dynamic interaction with the magnetosphere. IWF is Co-Investigator for the *Soft X-ray Imager (SXI)*, led by the University of Leicester, and the magnetometer *(MAG)*, led by CAS.

The institute, in close cooperation with international partners, contributes the instrument's control and power unit *EBOX* (figure below) for *SXI*. IWF is coordinating the development and design of the Digital Processing Unit (DPU) and is responsible for the mechanical design and the tests at box level. In 2018, IWF established the concept for the DPU prototype and completed the preliminary design of the box mechanics.

In addition to the hardware activities, IWF is participating in the science preparation such as modeling and in-situ science working group activities.

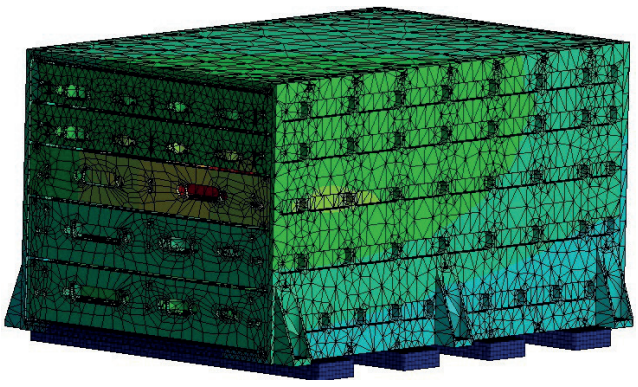

The results from the thermal analysis for the *SXI-EBOX* when closing the radiation protection for the CCD.

CSES

The China Seismo-Electromagnetic Satellites (CSES) are scientific missions dedicated to the investigation and monitoring of variations of electromagnetic fields and waves as well as plasma parameters and particle fluxes in the near-Earth space, which are induced by natural sources on ground like seismic and volcanic events.

After the successful launch of the first satellite *CSES-1* in February 2018, the second satellite *CSES-2 is* scheduled for launch in 2022. It will be in the same Sun-synchronous circular low Earth orbit as *CSES-1*, with a local time of the descending node at 2 pm, but with a phase difference of 180 degrees. The combined observations of both satellites will double the detection probability of natural hazard-related events and will help to separate seismic from non-seismic events.

The *CSES* magnetometers, which are nearly identical on both spacecraft, have been developed in cooperation between the National Space Science Center (NSSC), the Institute of Experimental Physics of Graz University of Technology (TUG), and IWF. NSSC is responsible for the dual sensor fluxgate magnetometer, the instrument processor and the power supply unit, while IWF and TUG participate with the newly developed absolute scalar magnetometer, called *Coupled Dark State Magnetometer (CDSM).*

Up to now, the magnetometer sensors of *CSES-1* operate continuously in good health and validation activities indicate a good data quality. In 2019, the data from *CSES-1* were e.g. used to compute the only geomagnetic field model up to degree and order of 15 in a spherical harmonic representation, which is independent from magnetic field data measured by ESA's *SWARM* mission.

GEO-KOMPSAT-2A

GEO-KOMPSAT-2A (GEOstationary KOrea Multi-Purpose SATellite-2A) is a South Korean meteorological and environmental satellite in geostationary orbit at 128.2° East which also hosts a space weather environment monitoring system. The implementation of the satellite, which was launched in 2018, and the necessary ground segment is managed by the Korean Meteorological Administration. The space weather observations aboard *GEO-KOMPSAT-2A* are performed by the Korean Space Environment Monitor (KSEM) which was developed under the lead of the Kyung Hee University. It consists of a set of particle detectors, a charging monitor and a four-sensor *Service Oriented Spacecraft MAGnetometer (SOSMAG).*

The *SOSMAG* development was initiated and conducted by ESA as part of the Space Situational Awareness Programme, and built by the *SOSMAG* consortium: IWF, Magson GmbH, Technische Universität Braunschweig and Imperial College London.

The *SOSMAG* instrument is a "ready-to-use" magnetometer avoiding the need of imposing magnetic cleanliness requirements onto the hosting spacecraft. This is achieved through the use of two high quality fluxgate sensors on an approximately one meter long boom and two additional magneto-resistive sensors mounted within the spacecraft body. The measurements of the two spacecraft sensors together with the inner boom sensor enable an automated correction of the outer boom sensor measurement for the dynamic stray fields from the spacecraft.

During the first year of operation it could be demonstrated that the four-sensor design enables a data quality, which is well within the mission requirements. The calibration, i.e. determination of the slowly-varying DC offsets of the spacecraft, is done at IWF through comparison of the AC-cleaned data with data calculated from the Tsyganenko model for actual solar wind parameters (obtained from the *WIND* spacecraft). The comparison is done in the physical reference frame of the geomagnetic field (Hp to North Pole, He to Earth center, Hn to East), such that the median values for each component of measured and model data coincide. The difference between the medians gives the DC offset for each component (figure below). In parallel to the flight data verification and calibration, the *SOSMAG* ground processor software has been under development in 2019. It shall be implemented in the data center of ESA's Space Safety program in 2020 for a nearly real time release of the *SOSMAG* data to the space weather community.

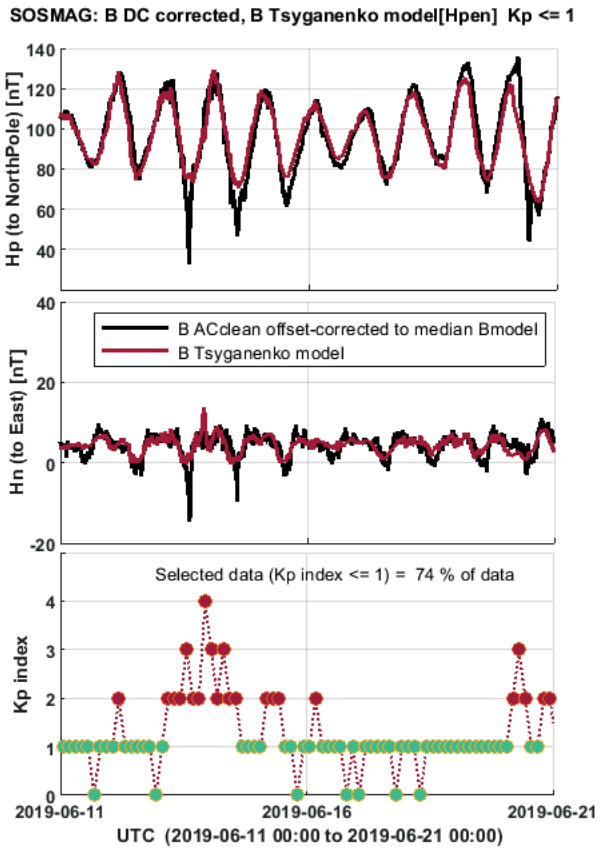

Example of the DC calibration for 10 days in June 2019. The correction with the DC offsets yields good results for times with Kp <= 1: the deviation between model data and DC corrected data is minimal. Stronger deviations are seen for times with disturbed magnetosphere (Kp > 1).

CALIBRATION OF MAGNETOMETERS ON SPIN-STABILIZED SPACECRAFT

Magnetometers are key instruments on board spacecraft that probe the plasma environments of planets and other solar system bodies. The linear conversion of raw magnetometer outputs to fully calibrated magnetic field measurements requires the accurate knowledge of 12 calibration parameters: six angles, three gain factors, and three offset values. The in-flight determination of 8 of those 12 parameters is enormously supported if the spacecraft is spin-stabilized, as an incorrect choice of those parameters will lead to systematic spin harmonic disturbances in the calibrated data. Unfortunately, previously published equations and algorithms for the determination of the eight spin-related parameters are far from optimal, as they do not take into account the physical behavior of science-grade magnetometers and the influence of a varying spacecraft attitude on the in-flight calibration. Thus, advanced calibration equations, parameters, and algorithms are introduced. A version of these algorithms is routinely applied to calibrate magnetometer data from *MMS*. With their help, it is possible to decouple different effects on the calibration parameters, originating from the spacecraft or the magnetometer itself. A key point of the algorithms is the bulk determination of parameters and associated uncertainties. Lowest uncertainties are expected under parameter-specific conditions, i.e., in specific regions. It is shown where these conditions are fulfilled in the near-Earth plasma environment.

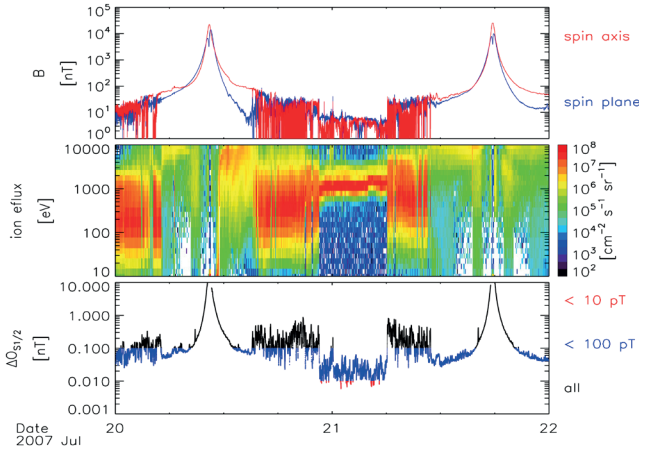

From top to bottom: magnitude of the spin axis and spin plane magnetic fields in red and blue, omnidirectional ion spectral energy flux density indicating different regions in near-Earth space, and uncertainties of the estimates of the spin plane offsets representing a group of calibration parameters.

ENERGY CONVERSION AT KINETIC SCALES IN THE MAGNETOSHEATH

The processes of converting or dissipating energy in nearly collisionless turbulent space plasmas are yet to be fully understood. Besides wave-particle interactions and non-resonant stochastic heating, (reconnecting) current sheets can contribute to irreversible energy dissipation in a turbulent space plasma environment. The terrestrial magnetosheath, downstream of a quasi-parallel bow shock, represents a turbulent region where the energy conversion associated with ion/electron scale current sheets can be studied. A statistical analysis based on high-resolution *MMS* measurements in the quasi-parallel magnetosheath revealed that properly defined and normalized energy exchange/dissipation measures, in average, increase with the current density (thick black line in the figure below). A similar trend was found in 2.5- and 3-dimensional turbulence Particle-In-Cell (PIC) simulations (green and magenta lines). The measure De in the figure corresponds to the work done by the electric field on particles without the transport term for the net charge. De was estimated in parallel (triangles) and perpendicular (circles) directions to the magnetic field. The results show that dissipation occurs preferentially in parallel directions, presumably because of the significant guide fields at current sheets in the quasi-parallel magnetosheath.

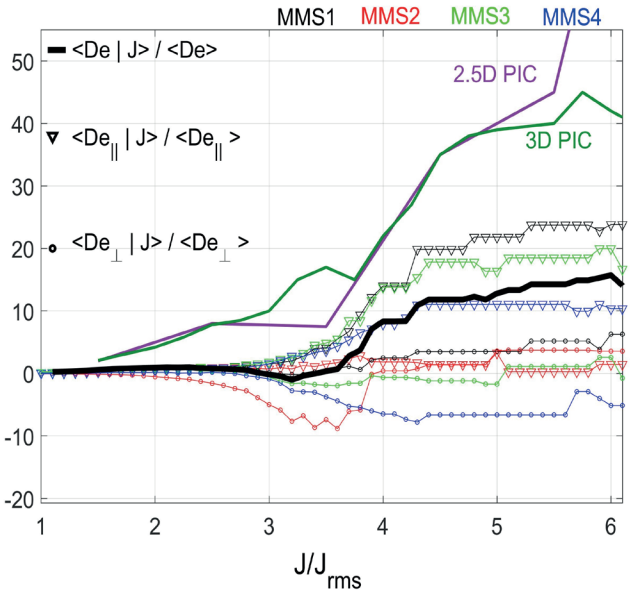

Normalized current density J/J_{rms} (rms = root mean square) versus conditional temporal averages of normalized energy conversion measure De, calculated by conditioning on the values of current density J. The color code corresponds to the spacecraft *MMS1-4*. The thick black line represents temporal and spatial averages of the normalized measure De between *MMS1-4* spacecraft. The green and magenta lines illustrate the results of the 2.5- and 3-dimensional turbulence PIC simulations.

CURRENT SHEET NEAR THE CENTER OF MAGNETIC RECONNECTION REGIONS

Magnetic reconnection is the process by which magnetic field lines coming from one region are broken and reconnected with magnetic field lines coming from another region. The simplest descriptions of magnetic reconnection are two-dimensional, and a number of theoretical predictions have been made using the two-dimensional assumption. Using multi-point data analysis techniques applied to an observation by the *MMS*, structures and evolution of a thin current sheet near the center region of magnetic reconnection are obtained and compared with these theoretical models. An agreement between the observations and the predictions of a two-dimensional theoretical model is found including the scale size of the reconnection region, details of the particle orbits, and the rate of reconnection. This agreement suggests that the scale size of the central region of reconnection, called "inner electron diffusion region", where the magnetic field is too small to make electrons gyrate around it, is determined by the thermal motion of the ambient electrons. It is shown that this non-gyrating feature of electrons is directly related to the rate of magnetic reconnection underpinning how reconnection works in a thin current sheet with quasi 2D geometry.

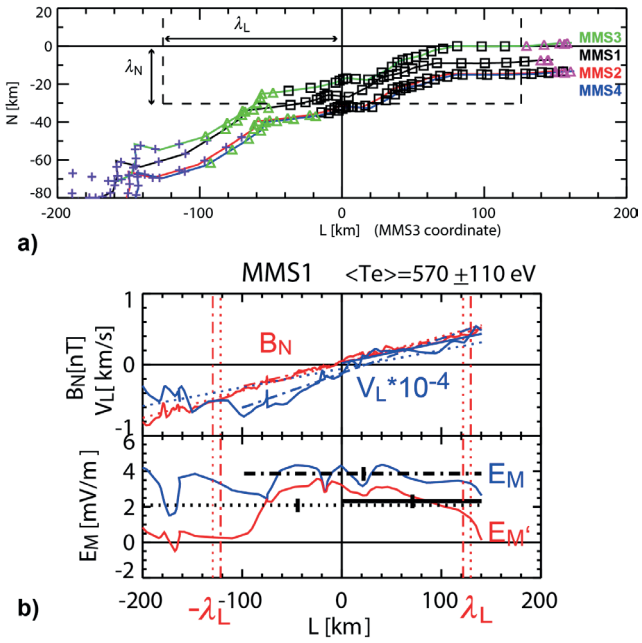

a) Location of the four spacecraft between 22:34:01.7-22:34:03.1 UT relative to the X-line. The colored symbols show the different types of electron velocity distribution function. b) Magnetic field, B_N (red) and electron flow velocity, V_L (blue) (upper panel) and electric field in spacecraft frame, E_M (blue) and electric field in electron frame $E_{M'}$ (red) (lower panel). Scale size of the center region is indicated by λ_L. The horizontal bars b) indicate the theoretical estimation of $E_{M'}$.

ELECTRON-SCALE PLASMA MIXING ON RECONNECTION SEPARATRICES

One of the natural consequences of reconnection is the mixing of plasma across a magnetic boundary. Mixing is often violent, and may have a significant impact on the reconnection process itself. For instance, narrow bands of high velocity electrons are frequently observed flowing toward the reconnection X-line along the separatrix dividing the larger scale inflow and outflow. It is suspected that the electric field required for acceleration is related to kinetic structures frequently observed in this region. One way to grow electric fields is by inflow and outflow electrons gyrating around the magnetic field such that they overlap at the separatrix, leading to thin, distinct layers of wave activity sandwiched between the magnetosphere and magnetosheath. Kinetic structures such as plasma double layers, however, are expected to form from a disturbance parallel to the magnetic field. For example, a head-on collision between the inflow and outflow may be set up by larger scale ripples frequently observed in the separatrix surface. To model this interaction, a numerical simulation was performed where two electron populations were allowed to mix and evolve. *MMS*-measured parallel electric fields from the separatrix region and corresponding data from the simulation are shown in the figure below. Despite their highly nonlinear nature, the largest amplitude features in $E_{||}$ were reproduced remarkably well, lending support for the parallel mixing model.

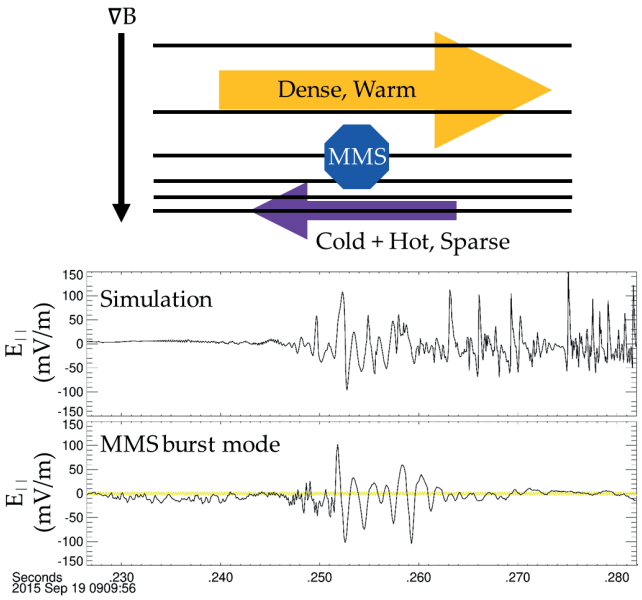

Schematic of *MMS* location relative to mixing electron populations. Central spike signatures of measured parallel electric fields are reproduced well by the simulation.

STABILITY & CHAOS OF ENSEMBLES IN MAGNETIC RECONNECTION REGIONS

Energetic outbursts on the Sun, like solar flares, and auroral substorms on Earth are two of several phenomena in space science that are driven by magnetic reconnection. This process of local recombination of magnetic field lines builds up stress in space plasma that accelerates particles, together with the field, and forms a shock front. The study of such non-collisional plasmas is impossible in laboratory experiments on Earth, and can only be done in space. Theoretical studies are necessary for the accurate interpretation of space-based measurements. Numerical simulations were used to better understand the topology of regions of regular and chaotic motions of plasma particles close to the reconnection site in the Earth's magnetotail. The theory of Lyapunov exponents, originally invented for single particle dynamics, was generalized to ensembles of plasma particles and successfully implemented in computer code to amend particle in cell simulations. Regions of strong and weak excitation of local perturbations in different plasma regions are found, and strong acceleration centers have been identified (see figure). The further analysis of chaos in space plasma may lead to a better understanding of the mixing behavior of plasma particles, i.e. the transformation of velocity distribution functions in different regions of Earth's magnetotail.

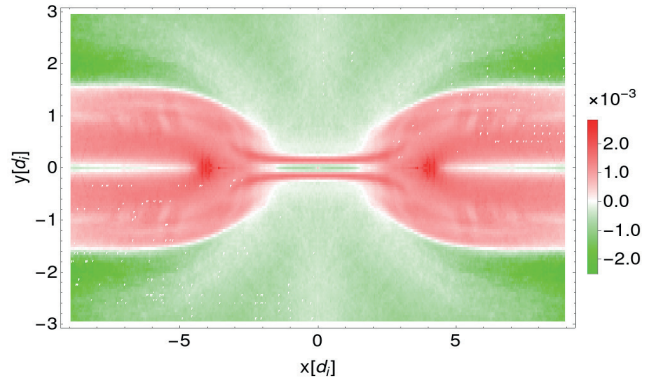

Mean Lyapunov Ensemble Number close to the reconnection center of Earth's magnetotail (color code: green - damping, red - excitation of local perturbations; normalized units of length, d_i, in configuration space x-y). Strong acceleration centers are shown in dark red.

IONOSPHERIC FOOTPRINTS OF DETACHED INTERCHANGE HEADS

The Earth's magnetotail periodically accumulates energy in the form of the magnetic flux in the tail lobes and dumps the energy as fast earthward and tailward plasma flows, which are produced by magnetic reconnection. Yet there is no consensus on what magnetotail processes may lead to reconnection. Examples of multiprobe space observations were used to reveal the possible process that might be important for azimuthally localized reconnection in the tail that leads to pseudo-breakups in aurora and local ionospheric current systems. The examples show the appearance of earthward-propagating reconnection (dipolarization) fronts amidst azimuthally propagating clumps of more dipolar field lines that were produced by an instability, which was predicted to lead to localized reconnection by earlier plasma computer simulations. The conjugate ground auroral and magnetic field observations support the fronts' origin hypothesis. In particular, using *THEMIS* observations in the plasma sheet and conjugate ground-based All-Sky-Imagers and ground magnetometer network observations, examples of prominent dipolarization fronts (DFs) were shown with moderate earthward flows that were observed amidst azimuthally drifting interchange heads at XGSM ≈ -11 R_E. The conjugate ground observations revealed ionospheric current intensifications and growth of auroral bright spots out of dimmer azimuthal beads/rays near *THEMIS* footprints. The DFs can be interpreted as separate Ballooning/InterChange Instability heads that detached from the region with reversed radial gradient of B_z and propagated earthward-driving ionospheric pseudo-breakups.

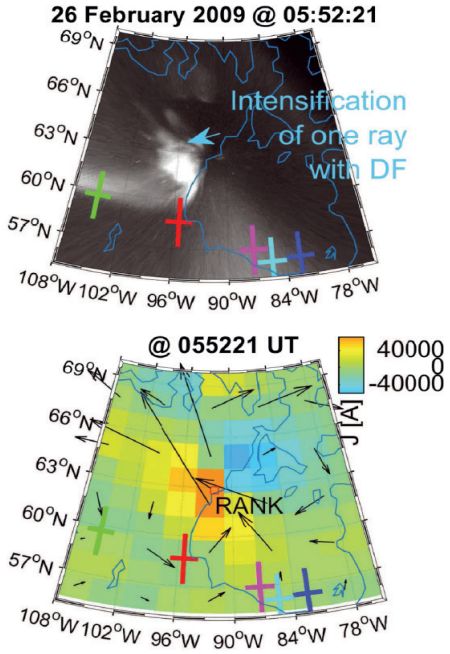

Snapshots from *THEMIS* Ground-Based All-Sky-Imager at Rankin Inlet, NU, Canada, and equivalent ionospheric current/Spherical Elementary Current System observations on 26 February 2009 during dipolarization front encounter by *THEMIS* at 5:52:21 UT.

3D STRUCTURE OF PLASMA FLUCTUATIONS AT ION KINETIC SCALES

Using *MMS*, the structure of plasma fluctuations in three dimensions was obtained for the first time. On 7 September 2015, the *MMS* spacecraft were located in the Earth's magnetosheath. During this interval the *MMS* spacecraft had separations of around 100 km before beginning their nominal mission with much smaller separations. The unique configuration of inter-spacecraft separations close to proton gyration scales and the exceptionally high time resolution of plasma data allow a much more detailed investigation of turbulence than was previously possible with the *Cluster* mission, where only magnetic and density data could be studied.

The results revealed that the temperature fluctuations as well as the velocity fluctuations have anisotropies with respect to the mean magnetic field direction similar to those in the magnetic field. The energy of the fluctuations for all parameters were found to decay faster in the direction of the mean magnetic field direction with respect to the perpendicular direction with the velocity fluctuations having the strongest anisotropy.

The figure shows the anisotropy of the spectral index for velocity fluctuations in the magnetosheath. The relation for the magnetic field has been explained theoretically and observed, however this is the first observation at ion kinetic scales of the other parameters. The fluctuation power was also found to decay faster in the ion velocity fluctuations when compared to magnetic fluctuations suggesting that the fluctuations in the magnetosheath are not related to slow mode like oscillations but rather to kinetic Alfvén wave oscillations. The observations presented here will allow theoretical predictions to be tested in future, to better understand the mechanisms of turbulent heating in the magnetosheath.

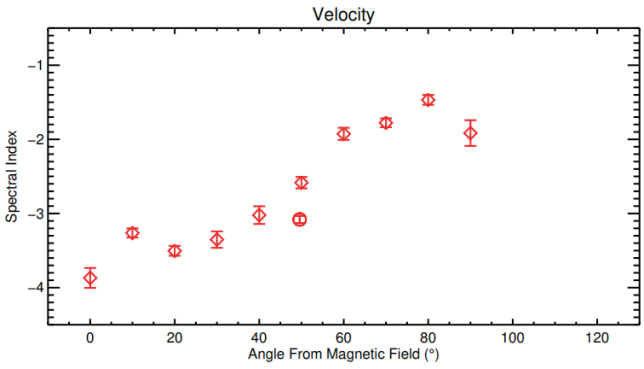

Variation of the spectral index of velocity fluctuations as a function of the angle from the mean magnetic field direction.

DISTURBANCE OF THE FRONT REGION OF RECONNECTION OUTFLOW JETS

Magnetic reconnection is a key process in collisionless plasmas that converts magnetic to plasma kinetic energy. The energy conversion in the reconnection process occurs in various locations in the reconnection layer. A new three-dimensional fully kinetic simulation of reconnection, whose system size is large enough to treat many of the important energy conversion locations, demonstrated that the energy conversion rate measured by $J \cdot E' = J \cdot [E + (V_e \times B)]$ in the front region of the reconnection outflow jets is comparable to that in the central reconnection region where the stored magnetic energy is first released (figure below). By applying a recently developed fully kinetic dispersion solver to parameters obtained from the simulation, it is confirmed that the strong energy conversion in the jet front region is led by the Lower-Hybrid Drift Instability (LHDI) induced by the sharp density gradient at the jet fronts. These results indicate that the LHDI fluctuations in the jet front region have a substantial effect on the energetics of reconnection. Interestingly, similar jet front fluctuations as seen in the simulation were observed by *MMS* on 18 July 2017. By applying the linear dispersion solver to this *MMS* event, it is confirmed that the jet front fluctuations in this *MMS* event are also driven by the LHDI, indicating the importance of the LHDI fluctuations in the Earth's magnetotail. Furthermore, by applying the linear dispersion solver to some other realistic parameter sets that cannot be handled by simulations and specific observation events, it is predicted that the LHDI fluctuations in the reconnection jet front region could occur over a wide parameter range in space plasma including the Earth's magnetotail and even solar flares.

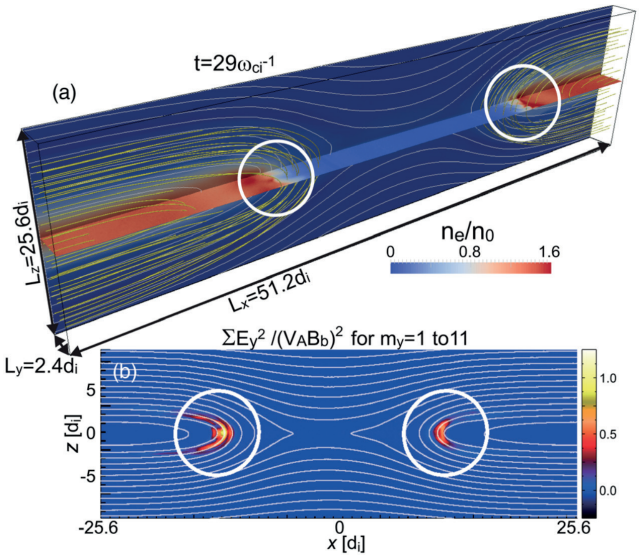

3D simulation results of (a) selected magnetic field lines near the jet fronts with density contours in the x-y plane at z=0 and x-z plane at y=0, and (b) integrated amplitudes of electric field (Ey) fluctuations in the y direction, highlighting the location of the LHDI fluctuations.

SOLAR SYSTEM

IWF is engaged in many missions, experiments and corresponding data analysis addressing solar system phenomena. The physics of the Sun and the solar wind, its interaction with solar system bodies, and various kinds of planetary atmosphere/surface interactions are under investigation.

SUN & SOLAR WIND

The Sun's electromagnetic radiation, magnetic activity, and the solar wind are strong drivers for various processes in the solar system.

SOLAR ORBITER

Solar Orbiter, launched in early 2020, is an ESA space mission to investigate the Sun. Flying a novel trajectory, with partial Sun-spacecraft corotation, the mission plans to investigate in-situ plasma properties of the inner solar heliosphere and to observe the Sun's magnetized atmosphere and polar regions.

IWF has built the Digital Processing Unit (DPU) for the *Radio and Plasma Waves (RPW)* instrument aboard *Solar Orbiter* and has calibrated the *RPW* antennas, using numerical analysis and anechoic chamber measurements. Furthermore, the institute has contributed to the magnetometer.

RPW will measure the magnetic and electric fields at high time resolution and will determine the characteristics of magnetic and electrostatic waves in the solar wind from almost DC to 20 MHz. Besides the 5 m long antennas and the AC magnetic field sensors, the instrument consists of four analyzers: the thermal noise and high frequency receiver; the time domain sampler; the low frequency receiver; and the bias unit for the antennas. The control of all analyzers and the communication will be performed by the DPU, developed by IWF.

Solar Orbiter removed from its shipping container at the Astrotech Space Operations Facility in Florida, US, on 18 November 2019.

HALL EFFECT IN SOLAR WIND TURBULENCE

Plasma and magnetic fields in space often develop into turbulence, for example in the freely-streaming solar wind and in the magnetopause region (boundary between the solar wind and the planetary magnetosphere). On smaller spatial scales, typically at length scale of 100 km, ions become inert and decouple from the electron motion, causing a Hall electric field in the plasma and leading to a Hall inertial range in plasma turbulence. A theoretical model of the Hall turbulence spectrum is proposed in a two-dimensional geometry perpendicular to the large-scale magnetic field. The Hall turbulence model gives a possible explanation for the steepening of the magnetic energy spectra in the solar wind, and can be tested against spacecraft measurements in the solar wind and planetary magnetopause region.

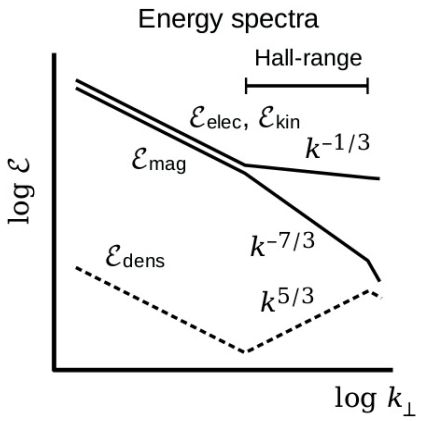

Spectra of the kinetic, electric, and magnetic energy, and density fluctuations in plasma turbulence in transition from magnetohydrodynamic behavior on smaller wavenumbers into Hall inertial range with steepening of magnetic energy and flattening of electric energy.

MERCURY

Mercury is in the center of attention because of the ESA/JAXA *BepiColombo* mission. The planet has a weak intrinsic magnetic field and develops a mini-magnetosphere, which strongly interacts with the solar wind.

BEPICOLOMBO

BepiColombo was launched from the European Spaceport in Kourou, French Guiana, aboard an Ariane-5 rocket in 2018. By the end of 2019 it has already traveled over one billion kilometers but still only covered about 12% of its voyage before arriving at Mercury at the end of 2025. Related, *BepiColombo* saw its first electric propulsion arc. Solar electric propulsion is one of the key flight challenges. 22 arcs will be necessary to let *BepiColombo* spiral closer to the inner solar system and finally reach the orbit around Mercury.

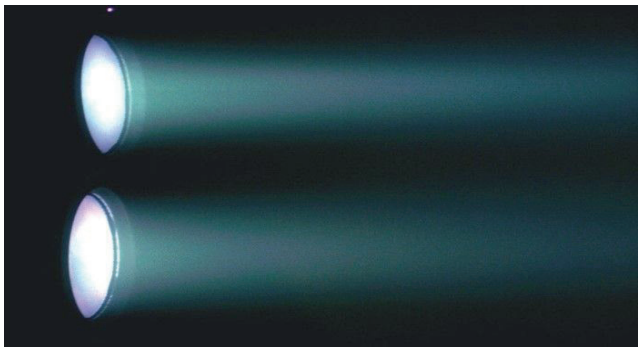

Two gridded ion thrusters as used on *BepiColombo* undergoing a joint test firing inside a vacuum chamber. In space the plumes seen here would not be visible; however, the glow from the thrusters would be visible (Credits: QineitQ).

An extensive series of in-orbit commissioning activities showed that the mission requirements as to overall capabilities and performance are met. In particular, the magnetic field sensors with IWF contribution are in very good health on both spacecraft, JAXA's *Magnetospheric (MMO)* and ESA's *Planetary Orbiter (MPO)*.

MMO-MGF (IWF PI-ship) with the two sensors on the still stowed boom was switched on only for a few hours during two health checks in May and December as well as during the very important release of the boom launch locks in August. The latter was postponed from November 2018 to mid-2019 because of the fact that the *MMO* spacecraft within the Sun shield is colder than originally expected.

MPO-MAG (IWF technical management) with the two sensors on the already deployed boom has been monitoring the magnetic field continuously except for the solar electric propulsion phase. Extensive calibration and data processing activities have since enabled to greatly decrease spacecraft-generated disturbances in the magnetic field observations; these activities constitute a key step towards making the data suitable for scientific analysis.

PICAM (IWF sensor PI-ship), the ion mass spectrometer with imaging capability as part of the *SERENA* instrument suite on *MPO*, underwent its high voltage commissioning in July 2019. The sensor is now technically verified. The first in-flight calibration will follow during the Earth flyby in 2020 by referring to the average plasma distribution and flux in the Earth's magnetosphere. A detailed planning was already required in 2019 to ensure both good measurements and the instrument's safety related to radiation.

MERCURY'S INTERNAL AND EXTERNAL MAGNETIC FIELDS

Mercury's magnetic field is considered to be complex. The planetary magnetosphere is so small and comparable to the size of the planet itself, so the external field from the currents flowing in the planetary magnetosphere has a significant influence even when measuring the field in the near-surface region. Identification of the internal and external magnetic fields in Mercury's magnetosphere is one of *BepiColombo*'s scientific goals. A novel data analysis method is being developed for the *BepiColombo* magnetometers. The method is based on an algorithm of nonlinear minimum variance projection developed for wave studies in space plasma, and can identify various sources from the spatially sampled magnetic field data in Mercury's magnetosphere. The analysis method was successfully tested against a synthetic two-spacecraft data set assuming an internal dipolar magnetic field and an external field from a planar magnetopause current on the dayside. In contrast to the conventional spherical harmonic analysis, the novel method can decompose the magnetic fields into various origins even if the currents are flowing or external fields are significant in the measurement. This innovative method opens the door to diagnose both the planetary internal structure and the current pattern in the planetary magnetosphere using *BepiColombo's* magnetic field data.

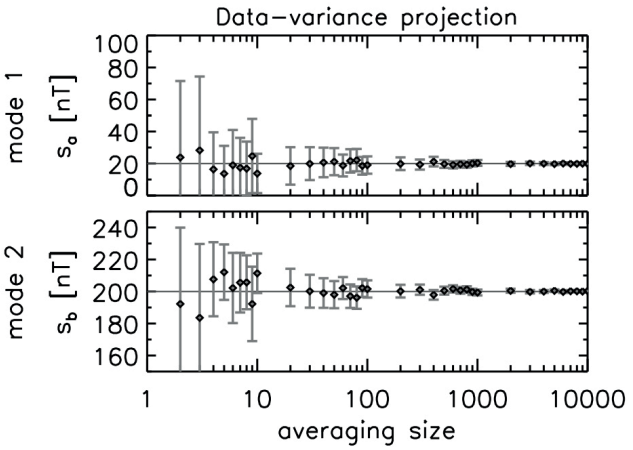

External magnetic field (mode 1) and internal dipolar magnetic field at the planetary surface (mode 2) plotted as a function of averaging size for the statistics. The mode amplitudes are obtained from the synthetic data modeled for the *BepiColombo* magnetometer on the dayside of Mercury using the nonlinear data-variance projection.

VENUS AND MARS

Venus and Mars are the Earth's nearest inner and outer neighbors, respectively. Venus orbits the Sun at 0.7 AU in 224 days, has a radius slightly smaller than the Earth, and has a very dense atmosphere. Mars orbits the Sun at 1.5 AU in 687 days, has about half the radius of the Earth, and has a very tenuous atmosphere. Both planets do not have an internal magnetic field, although Mars does show remnant surface magnetization, which might indicate that the planet used to have a functioning dynamo. Through their interaction with the solar wind, however, a so-called induced magnetosphere is created around each planet.

CHINA MARS EXPLORATION MISSION

China's Mars orbiter, lander, and rover mission is ready for launch in 2020. The main mission will conduct a comprehensive remote sensing of the Red Planet, as well as surface investigation. IWF contributed to a magnetometer aboard the orbiter.

China Mars Exploration Mission in launch configuration, with the orbiter and lander/rover inside the heat shield (top), undergoing thermal vacuum testing (© CAS).

INSIGHT

NASA's Mars mission *InSight (INterior exploration using Seismic Investigations, Geodesy and Heat Transport)* successfully landed in Elysium Planitia in 2018. The *Heat flow and Physical Properties Probe (HP³)* was designed to measure the internal heat flux of Mars as well as the thermal and mechanical properties of the Martian regolith. In order to describe the penetration progress and to derive soil mechanical parameters for the first couple of meters of the regolith, two numerical models have been developed at IWF. In February 2019, the "Mole" started hammering itself into Martian ground but got stuck only after about 30 cm, caused by lacking friction of the Martian sand. Even though assistance by *InSight's* scoop was successful, it is not certain whether the "Mole" will go deeper by itself. However, even in the numerical model it could be demonstrated that the first half meter is the most difficult part of the insertion process.

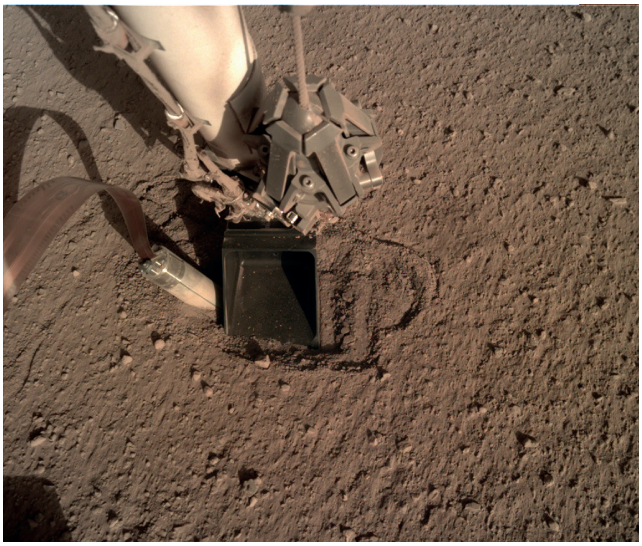

InSight's robotic arm used its scoop to pin the "Mole" against the wall of its hole (© NASA/JPL-Caltech).

TESTING OF EXOMARS ROVER SAMPLING SYSTEM

ESA's *ExoMars* rover, due for launch in 2022, is part of a mission addressing the question of whether life has ever existed on Mars. Therefore, the rover is equipped with a drill, to create boreholes to a maximum depth of 2 m and to take core samples within the drill's range. In order to facilitate the chemical analysis of the Martian ground, the retrieved drill cores must first be milled. This task is performed by a crushing station (CS), which delivers the milled sample material to a dosing device (PSDDS). From there the material is distributed further to the analysis instruments. To demonstrate the proper functionality of the CS and the PSDDS laboratory tests under simulated Mars conditions were performed in the Surface Laboratory at IWF. The focus was on the investigation of the effects of cementation in Martian regolith on the performance of the system.

JUPITER AND SATURN

Jupiter and Saturn are the two gas giants in our solar system at a distance of 5.2 and 9.5 AU, respectively. Both planets have strong inner magnetic fields and rotate rapidly with a day lasting around 10 hours. Consequently, they have rotationally dominated magnetospheres and are strong radio sources in the sky. Jupiter has four large moons (but 79 in total), Io, Europa, Ganymede and Callisto. Of these four, Ganymede is the target moon for the upcoming *JUICE* mission. Saturn has 82 moons of which two have been studied in great detail: Titan was the target for the *Huygens* probe and Enceladus has shown to eject water and is expected to have an ocean under its icy surface.

JUICE

ESA's first large (L-class) mission *JUpiter ICy moons Explorer (JUICE)* is planned to be launched in June 2022 and to arrive at Jupiter in late 2029, starting a 3.5 years discovery mission. It will make detailed observations of the gas giant and three of its largest moons, Ganymede, Callisto, and Europa. These three moons are thought to have water oceans below their icy surfaces. Towards the end of the mission it will orbit Jupiter's largest moon Ganymede. Currently, ESA and the prime contractor Airbus are testing the engineering models, and the assembly of the flight model has also begun.

The *Jupiter MAGnetometer (J-MAG)* is led by Imperial College London and will measure the magnetic field vector and magnitude in the bandwidth DC to 64 Hz in the spacecraft vicinity. It is a conventional dual sensor fluxgate configuration combined with an absolute scalar sensor based on more recently developed technology. Science outcome from *J-MAG* will contribute to a much better understanding of the formation of the Galilean satellites, an improved characterization of their oceans and interiors, and will provide deep insight into the behavior of rapidly rotating magnetic bodies. IWF supplies the atomic scalar sensor for *J-MAG*, which is developed in collaboration with TU Graz. In 2019, the qualification model was finished and delivered to IC London for environmental testing. The acceptance tested optical fibers have already been integrated on the 10.5 m long flight boom and the manufacturing of the flight instrument has been started.

The *Particle Environment Package (PEP)* is a plasma package with sensors to characterize the plasma environment of the Jovian system and the composition of the exospheres of Callisto, Ganymede, and Europa. IWF participates in the *PEP* consortium on Co-Investigator basis in the scientific studies related to the plasma interaction and exosphere formation of the Jovian satellites.

IWF is also responsible for the calibration of the radio antennas of the *Radio and Plasma Wave Investigation (RPWI).* In 2019, additional numerical antenna simulations were performed to estimate the influence of the radar antenna on the *RPWI* sensors. It was found that the strong radar pulses with a radiated power of 10 W will saturate the radio antenna receiver, not allowing scientific measurements at the same time.

DYNAMICS OF SATURN LIGHTNING STORMS

NASA's *Cassini* mission orbited the gas giant Saturn for more than 13 years (2004-2017). It has provided a wealth of scientific data that will keep scientists busy for several more years.

A combined analysis of data from *Cassini's RPWS (Radio and Plasma Wave Science)* instrument together with images from the *Cassini* cameras and from ground-based amateurs has revealed new clues about the dynamics of Saturn's lightning storms. It suggests that decreases in the flash rate are caused by the splitting of the thunderstorm into a bright cloud and a dark oval. These dark ovals drift westward as can be seen in the image below.

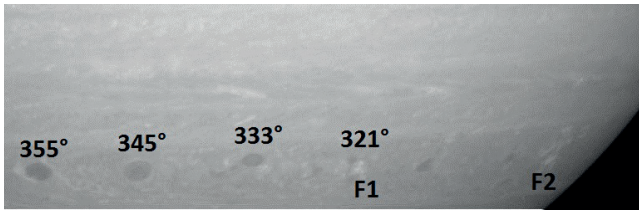

Saturn's storm alley around 35° South latitude imaged by the *Cassini* camera on 23 April 2008. The two bright features F1 and F2 are thunderstorm cells, which have spawned several dark ovals, indicated by their western longitudes.

Cassini RPWS detected about 277 000 lightning strokes in 439 episodes during this storm that lasted for 7.5 months from November 2007 until July 2008. Another comparison with images showed that lightning radio emissions can already be detected when the storm is still beyond the visible horizon. This so-called over-the-horizon effect was found to mainly occur when the storm is on the night side and the observer *Cassini* on the day side. It is thought to be due to a temporary trapping of the radio waves below Saturn's ionosphere.

A test version of the 10.5 m long magnetometer boom for *JUICE* at ESA's Test Center ESTEC in the Netherlands, its weight borne by balloons (© ESA–G. Porter).

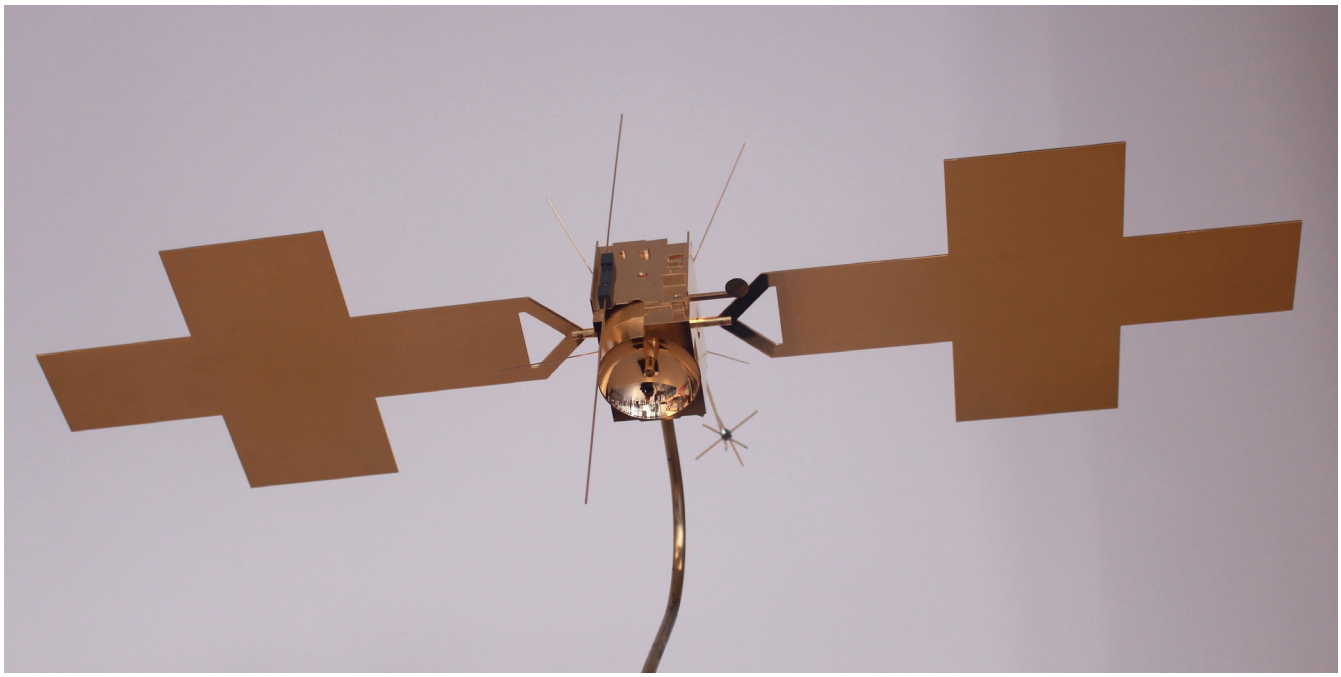

The miniature gold-plated metallic model of *JUICE*, used to test the spacecraft's antennas, was ESA's Space Science Image of the Week in November 2019.

COMETS AND DUST

Comets and dust are the remains of the planetary cloud surrounding the new-born Sun, from which the planets were created. Although, dust can also be created at a later stage through collisions of e.g. asteroids. ESA's *Rosetta* mission to comet 67P/Churyumov-Gerasimenko restarted the interest in in-situ cometary physics and will be followed up by ESA's first fast (F-class) mission *Comet Interceptor*.

COMET INTERCEPTOR

The mission's primary science goal is to characterize, for the first time, a dynamically-new comet or interstellar object, including its surface composition, shape, structure, and the composition of its gas coma. It will consist of three spacecraft, which will give a unique, multi-point "snapshot" measurement of the comet - solar wind interaction region, complementing single spacecraft observations made at other comets.

A new comet, fresh from the Kuiper belt or the Oort cloud, is to be spotted by Earthbound telescopes, its ephemeris determined and then selected as a target if it crosses the ecliptic at an appropriate distance from the Earth. If available, an interstellar object like 1I/'Oumuamua or 2I/Borisov, can also be defined as a target.

Comet Interceptor will be launched with ESA's *ARIEL* spacecraft in 2028.

Comet Interceptor logo.

DYNAMIC FIELD LINE DRAPING AT COMET 67P/CG

The *Rosetta* dayside excursion took place in September–October 2015 when comet 67P/Churyumov-Gerasimenko (67P/CG) was located at ~1.36 AU from the Sun after it had passed perihelion on 13 August 2015 at ~1.25 AU. At this time, the comet was near its most active period, and its interaction with the solar wind was expected to be at its most intense, with ion pickup and magnetic field line draping.

The data from the *Rosetta Plasma Consortium (RPC)* were used to investigate the interaction of solar wind and comet. Calculating the cone, clock angle, and draping pattern of the magnetic field around the comet's nucleus was determined.

The cone angle changed several times, which means that the magnetic field direction changes from pointing sunward to anti-sunward as shown in the figure below. This is caused by the changing directions of the interplanetary magnetic field that is transported toward the comet. The cone-angle direction shows that mass-loading of the interplanetary magnetic field of the solar wind leads to dynamic draping. The ion velocity and the magnetic field strength are correlated because the unmagnetized ions are accelerated more (less) strongly by the increasing (decreasing) magnetic field strength. *Rosetta RPC* has shown that (dynamic) draping also occurs at mildly active comets, as was found at highly active comets such as 1P/Halley and 21P/Giacobini-Zinner, but also that determining both dynamic and nested draping will require a combination of fast flybys and slow excursions for future missions.

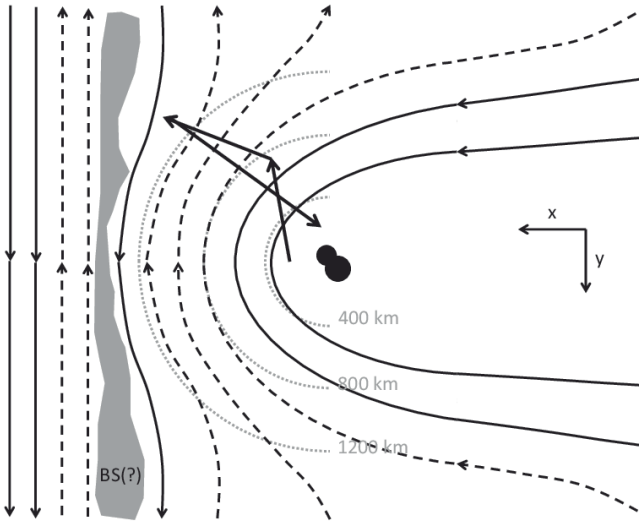

The draped magnetic field around 67P/CG. The three arrows in the figure illustrate the path of *Rosetta* during the dayside excursion.

COMETARY DUST AT THE NANOMETER SCALE

The *MIDAS* atomic force microscope on board the *Rosetta* orbiter collected and imaged µm-sized dust particles of comet 67P/Churyumov-Gerasimenko. *MIDAS*' dataset contains 3D images of structurally minimally altered, µm-sized cometary dust particles. Its investigation contributes to the understanding of our early solar system.

MIDAS data analysis at the µm scale already revealed cometary dust as hierarchical. The figure below shows a cometary particle of 1 µm size scanned with a resolution of 8 nm. Its structure continues the typical hierarchical agglomerate structure where the smallest identifiable features are of 100 nm size shape and of about 400 nm sized for clusters. The smallest features are of bulbous shape, their sizes follow a log-normal size distribution with a mean of about 100 nm and a standard deviation between 20 and 35 nm.

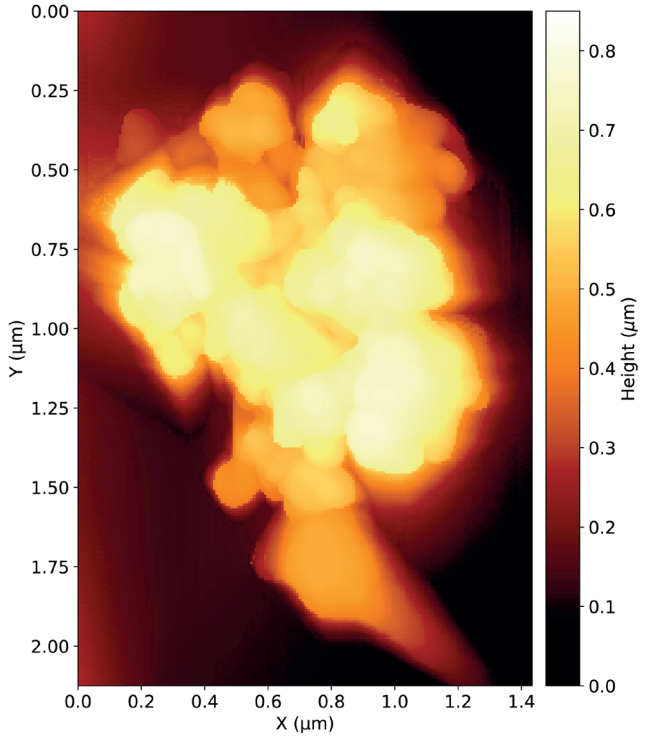

A 1 µm sized particle scanned with *MIDAS* showing the typical hierarchical structure of cometary dust. It consists of about 100 nm sized subunits clustering into about 400 nm sized structures.

Cometary material suitable for comparison are Chondritic Porous Interplanetary Dust Particles (CP IDPs). Their fundamental building blocks show subunit size distributions, shapes, and arrangements similar to that of *MIDAS* particles. This strengthens the link between CP IDPs and comets, and indicates that the smallest subunits identified by *MIDAS* could be the fundamental building blocks of comet 67P/CG.

TEMPORARY CAPTURE OF CHARGED DUST IN THE OUTER HELIOSPHERE

It is well known that cometary activity is one of the major sources for the production of micron-sized dust in the heliosphere (besides collisions of minor planets and dust streams from the interstellar medium). Several space missions to comets, like *Rosetta*, have revealed a deeper understanding of cometary dust in the inner part of the heliosphere. The origin, life-time and composition of dust grains in the outer parts of the solar system is currently less known and the scientific progress in this research field strongly relies on pure theoretical studies. A better understanding of dust grain dynamics will not only affect the interpretation of recent measurements in the outer heliosphere (e.g. *New Horizons*), but also help to design the next generation instruments aboard future space missions to the outer planets (i.e. *MUSE*). In a recent study it has been found that dust grains with specific charge-to-mass ratios (see figure) can be trapped at specific distances from the Sun for long times due to their interaction with planet Jupiter. Their orbital life time is increased despite the perturbations from non-gravitational effects, due to radiation, the interplanetary magnetic field, and interactions with the solar wind. To conclude, dust density enhancements in the solar wind are more likely to exist in the outer solar system than it was previously thought.

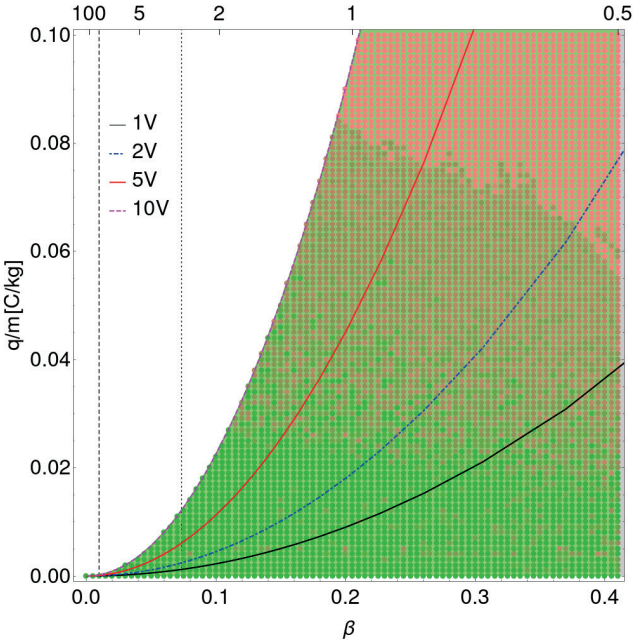

Probability of temporary capture (green: high, red: low) of dust with specific charge-to-mass ratios q/m versus solar radiation efficiency factor β, being inverse proportional to dust grain radius in micrometers (provided at the top of the figure).

HEAT BALANCE ON COMETARY SURFACES

The heat flow on cometary surfaces due to solar illumination is a dominant factor of influence on all physical processes on the surface of comets. In this context, it is usually assumed that only the flow normal to the surface is of importance and that lateral flows (tangential to the surface) are negligible. This conjecture was investigated by numerical simulations for two spots on comet 67P/Churyumov-Gerasimenko which were observed by the *MIRO* instrument aboard the *Rosetta* orbiter. For this purpose, the temperature evolution due to insolation and heat flow in the upper subsurface regions was calculated and the results compared with the *MIRO* observations. The figure below shows the temperature distribution on the region surrounding spot 1 for the observation time, and for quarters of the comet rotation later. The black and yellow circle indicate the spot sizes for the two channels (mm- and submm-wavelength) of the *MIRO* instrument.

It was found that lateral heat flow is, on average, very weak. However, at shadow margins it can be responsible for considerable temperature offsets of 10 K or more from the purely normal heat flow regime. Since the surface is very rough with asperities ranging from micrometer to meter size, shadow margins are distributed densely over the sunlit part of the surface. Therefore, it cannot be ruled out that lateral heat flow plays a significant role in other physical processes going on in the uppermost surface layers.

An integration of the radiated thermal emissions throughout the respective spots enables a comparison with the actual *MIRO* measurements. Very good agreement was found for the mm, but a significant deviation for the submm wavelength. Since the two different wavelengths have different penetration depths (4 and 1 cm, respectively), these results are an indication of the heterogeneity of the uppermost subsurface region of a few centimeters depth. Potential origins have been identified for the submm discrepancy, in particular surface roughness, thermal conductivity discontinuity and sublimation of water ice with consequential gas flow.

Temperature evolution around a spot on comet 67P/CG, observed by *Rosetta/MIRO*.

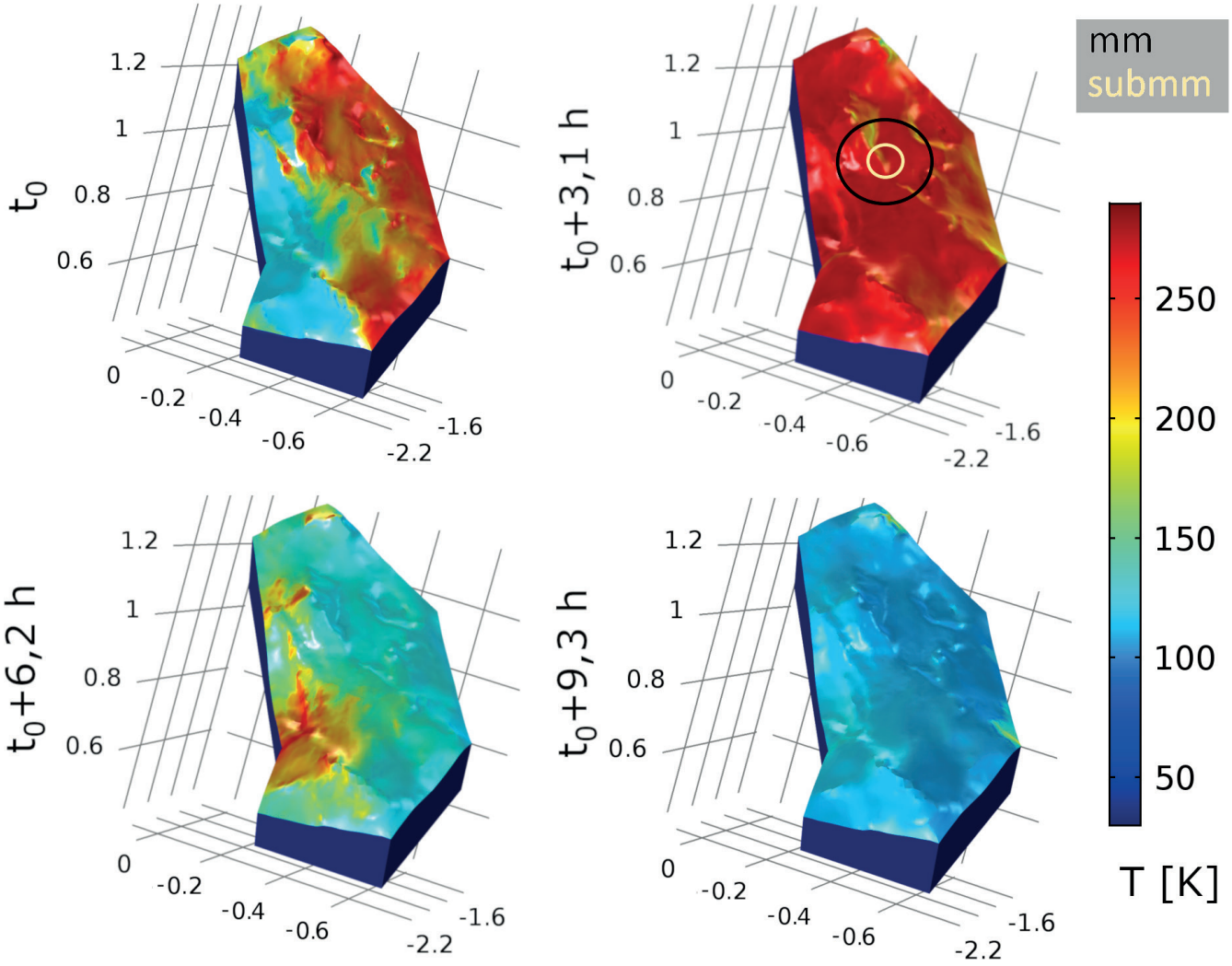

EXOPLANETARY SYSTEMS

The field of exoplanet research (i.e. investigation of planets orbiting stars other than the Sun) has developed strongly in the past decades. Since the discovery of 51 Peg b in 1995, the first detected exoplanet orbiting a Sun-like star, about 4500 exoplanets, most in planetary systems, are now known. Improved instrumentation and analysis techniques have led to the detection of smaller and lighter planets, down to Earth-size, Earth-mass planets, some orbiting in the habitable zone of the cooler stars. However, hot Neptunes and (ultra-)hot Jupiters are now prime targets for atmospheric characterization, mostly because of their larger radii, which indicate the presence of a volatile-rich atmosphere and facilitate observations and analyses.

The main exoplanet missions with IWF contributions are *CHEOPS*, *CUTE*, *PLATO*, and *ARIEL*. *CHEOPS* will precisely measure the radii of already known planets to greatly improve their inferred density and hence provide a first characterization. *CUTE* will obtain low-resolution near-ultraviolet transmission spectra of transiting giant planets to study upper atmospheres and mass loss processes. *PLATO* will look for planets in large portions of the sky, with the primary aim to find Earth-like planets in the habitable zone of Sun-like stars. *ARIEL* will collect low-resolution infrared transmission spectra of transiting planets to characterize planetary atmospheres, with the final goal of measuring C and O abundances, which constrain planet formation theories.

IWF concentrates on the study and characterization of planetary atmospheres using both theory and observations, focusing particularly on the analysis of exoplanet atmospheric escape and mass-loss processes. Further research is conducted to study star-planet interaction and carry out atmospheric characterization through the collection and analysis of ground- and space-based observations.

Exoplanet mission timeline (© ESA).

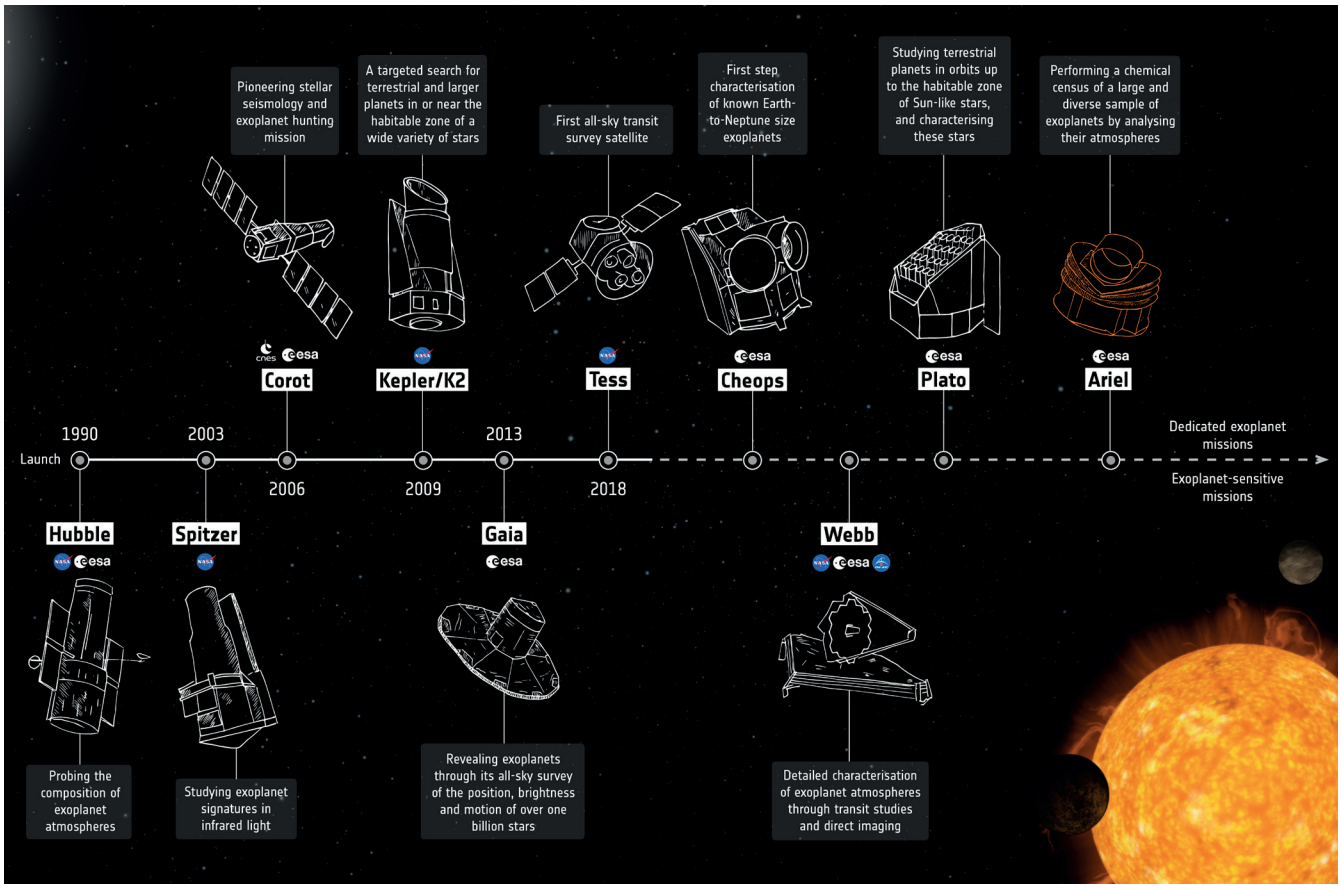

CHEOPS

CHEOPS (CHaracterising ExOPlanet Satellite), successfully launched on 18 December 2019, will study extrasolar planets and observe planetary systems at an unprecedented photometric precision. The main science goals are to detect transits of small planets, known to exist from radial-velocity surveys, precisely measure planetary radii to study the nature of Neptune- to Earth-sized planets, and obtain precise observations of transiting giant planets to study their atmospheric properties. IWF provided the *Back-End-Electronics (BEE)*, one of the two on-board computers, which controls the data flow and the thermal stability of the telescope structure. The institute was also responsible for the planning of two observing programs within the Guaranteed Time Observations of the *CHEOPS* consortium.

ARIEL

ARIEL (Atmospheric Remote-sensing Infrared Exoplanet Large-survey) is ESA's fourth medium (M-class) mission, led by University College London, to be launched in 2028. It will investigate the atmospheres of several hundreds exoplanets to address the fundamental questions on how planetary systems form and evolve. During its four-year mission, *ARIEL* will observe 1000 exoplanets ranging from Jupiter- and Neptune- down to super-Earth-size in the visible and infrared with its meter-class telescope. The analysis of *ARIEL* spectra and photometric data will enable extracting the chemical fingerprints of gases and condensates in planetary atmospheres, including the elemental composition for the most favorable targets, with a particular focus on carbon and oxygen. Thermal and scattering properties of the atmosphere will also be studied.

ARIEL consists of a one meter telescope feeding two infrared low-resolution spectrographs and the fine guiding sensor (FGS), working in the optical. To improve the satellite's pointing stability, the FGS provides optical photometry of the target in three broad bands that are used to control instrumental systematics, measure intrinsic stellar variability, and constrain the presence of high-altitude aerosols in planetary atmospheres. Within the *ARIEL* mission, IWF co-leads the upper atmosphere working group and is heavily involved in testing the mission's performances and advancing the atmospheric retrieval tools.

Academy President Anton Zeilinger (second from right) welcomes Federal Ministers Andreas Reichhardt, Iris Rauskala, IWF Director Wolfgang Baumjohann, and head of FFG/ALR Andreas Geisler (from left to right) to the *CHEOPS* Launch Event at ÖAW in Vienna.

CUTE

CUTE (Colorado Ultraviolet Transit Experiment) is a NASA-funded 6U-form CubeSat led by the University of Colorado and scheduled for launch in December 2020. It will perform low-resolution transmission spectroscopy of transiting extrasolar planets at near-ultraviolet wavelengths. *CUTE* will study the upper atmosphere of short period extrasolar planets with the aim of observationally constraining atmospheric escape processes, which are key to understand planetary evolution, and detect heavy metals, which constrain the presence and composition of aerosols in the lower atmosphere. Furthermore, *CUTE*'s continuous temporal coverage of planetary transits will allow to detect transit asymmetries, which are possibly connected with the presence of planetary magnetic fields.

IWF is the only technological contributor to the mission outside of the University of Colorado (Boulder), where *CUTE* is being developed. IWF is responsible for the development of the data simulator and ground data reduction software, and for the definition of the on-board data reduction software.

In 2019, IWF has finalized the development of the *CUTE* data simulator, which is a set of IDL routines generating images that reproduce spectral time series of stars taking into account the wavelength-dependent planetary absorption during transit and instrumental effects. The simulator recreates the effects that CCDs (e.g., size, pixel scale, and cosmetics), readout electronics, optical elements (telescope and spectrograph), planetary absorption during transit, spacecraft orientation and jitter, and systematic noise sources have on the data. This allows the user to best foresee the data quality and the magnitude of different sources of noise (both white and red).

The simulator is fed by a wide range of input parameters providing high flexibility. It follows that the simulator, which is originally designed for *CUTE*, can be easily adapted to work for any other mission carrying on-board a long-slit spectrograph and a charge transfer device as detector.

The simulator has been used to estimate the precision on the transit depth, in %, that will be obtained with *CUTE* by integrating over four different wavelength regions as a function of magnitude and effective temperature of the host star (see figure). Two of the four selected wavelength ranges are broad and cover the region with the highest stellar flux in the *CUTE* band (i.e., above 3000 Å) and the region below 2700 Å, which has been shown to be also sensitive to exoplanet atmospheric escape. The other two regions are centered on the MgII h&k resonance lines and the MgI resonance line at 2852 Å. It has been found that the uncertainty on the transit depth decreases with increasing stellar temperature and decreasing magnitude. Considering an average transit duration of 2.5 hours, without gaps over one transit the precision on the transit depth improves by a factor of about five. At the wavelengths of lines probing atmospheric escape, transit depths are typically larger than 2-3%. Therefore, within a few transits *CUTE* will be capable of detecting escape for planets orbiting stars brighter than the 13th magnitude and hotter than about 6500 K. For cooler stars, the detection of atmospheric escape will be limited to the brighter ones, such as the hot Jupiter HD189733, for which reaching the necessary precision will require the observation of about 10 transits. The case of the ultra-hot Jupiter KELT-9 is particularly remarkable as within a single transit *CUTE* will be able to reach a precision on the transit depth at the position of the MgI and MgII lines of about 0.1%. This translates to a precision on the planetary radius of about 2.2%, which corresponds to about two pressure scale heights.

Left: Uncertainty on the transit depth, in %, for a five minutes *CUTE* observation integrating in wavelength above 3000 Å.
Middle: Same as left panel, but integrating in wavelength around the MgII h&k resonance lines (2790-2810 Å).
Right: Same as left panel, but integrating in wavelength around the MgI resonance line (2850-2854 Å).
Each panel marks also the position of some of the systems for which signatures of atmospheric escape have been observed in the past. The results account for the effects of spacecraft jitter.

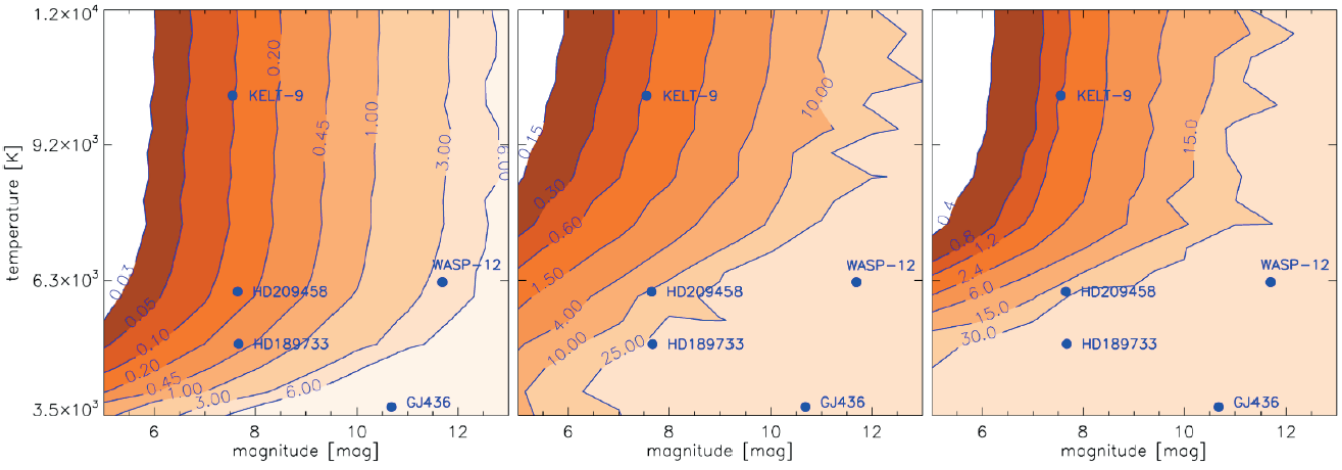

PLATO

PLATO (PLAnetary Transits and Oscillations of stars) is ESA's third medium (M-class) mission, led by DLR. Its objective is to find and study a large number of extrasolar planetary systems, with emphasis on the properties of terrestrial planets in the habitable zone around solar-like stars. *PLATO* has also been designed to investigate seismic activity of stars, enabling the precise characterization of the host star, including its age. IWF contributes to the development of the I*nstrument Controller Unit (ICU)* with the development of the *Router and Data Compression Unit (RDCU)*. Launch is expected in 2026. *PLATO* consists of 24 telescopes for nominal and two telescopes for fast observations. Each telescope has its dedicated front-end-electronics, reading and digitizing the CCD content. Six nominal and two fast DPUs collect the data from the front-end-electronics and extract the areas of interest. The *RDCU* is a key element in the data processing chain, providing the communication between the DPUs and the *ICU*. The second task of the *RDCU* is the lossless compression of the science data. For performance reasons, the compression algorithm is implemented in an FPGA.

Main tasks in 2019 were the design of the *RDCU* engineering model, the continuation with the design of the VHDL code and the development of the test environment. The design of the compressor has been further optimized to comply with the increased number of imagettes, from ~18000 to ~28000. An improved concept for the data transfer is under development to gain another 20% in performance. The *RDCU* design is compliant with all requirements and ready for manufacturing the engineering models.

OTHER TELESCOPES

Members of the institute obtained 10 nights of observing time with the *ESPRESSO* instrument at the *Very Large Telescope (VLT)* at the Paranal site of the European Southern Observatory (ESO), in Chile. These spectroscopic observations will be used in conjunction with *CHEOPS* observations to study the effect of stellar activity on radial velocity measurements and in turn identify possible ways of correcting radial velocity/photometric measurements using photometric/radial velocity observations.

Artist's impression of *PLATO* on its way to Lagrange Point 2 (L2). Here, the spacecraft is shielded from the Sun and has a clear view of the whole sky (© OHB System AG).

CLOSE-IN SUB-NEPTUNES REVEAL ROTATION HISTORY OF HOST STARS

Planet atmospheric escape induced by high-energy stellar irradiation shapes the structure and evolution of planetary atmospheres. Therefore, the present-day properties of a planetary atmosphere are intimately connected with the amount of stellar flux received by a planet during its lifetime, thus with the evolutionary path of its host star. A Bayesian framework has been developed and employed to track the evolution of planets as a function of stellar flux evolution history, constrained by the measured planetary radius. The tool has been tested on a large number of synthetic systems identifying the framework's validity range and that the ideal objects for this type of study are close-in sub-Neptune-like planets. Such planets are highly affected by atmospheric escape, and yet retain a significant fraction of their primordial H-dominated atmospheres. The algorithm has been applied to the HD3167 and K2-32 planetary systems. For HD3167, the most probable irradiation level at 150 Myr has been found to lie between 40 and 130 times solar, corresponding to a rotation period of $1.78^{+2.69}_{-1.23}$ days. K2-32 had a surprisingly low irradiation level ranging between half and four times solar at 150 Myr. For multi-planet systems, the analysis framework enables one to constrain poorly known properties of individual planets, such as planetary masses.

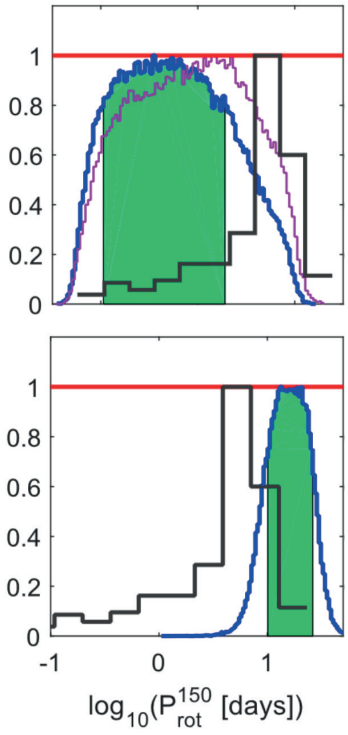

Markov-chain Monte Carlo (MCMC) posterior distributions for the stellar rotation period at an age of 150 Myr obtained from the modeling of HD3167c (top) and K2-32b (bottom). The shaded areas correspond to the 68% highest posterior density (HPD) credible interval. In the upper panel, the blue and violet distributions are for two different sets of system parameters. The red line shows the assumed prior. The black line histogram shows the distribution of rotation periods for young open cluster stars with masses between 0.8 and 0.9 solar masses.

KEPLER-11: HIGH-ENERGY EMISSION AND ATMOSPHERIC MASS FRACTIONS

The atmospheres of close-in planets are strongly influenced by mass loss. It has been shown that the framework enabling the recovery of the past evolution of the stellar high-energy emission from the present-day properties of its planets can also provide constraints on planetary initial atmospheric mass fractions. The constraints on the output parameters improve when more planets can be simultaneously analyzed, making the Kepler-11 system, which hosts six mini-Neptunes, an ideal target. The results indicate that the star has likely evolved as a slow rotator (slower than 85% of the stars with similar masses), corresponding to a high-energy emission at 120 Myr of between 1-10 times that of the current Sun (see figure). The derived planetary initial atmospheric mass fractions are <4.1% for planet c, 3.7-5.3% for planet d, 11.1-14% for planet e, 1-15.6% for planet f, and 4.7-8.7% for planet g assuming a disc dispersal time of 1 Myr. For planet b, the range remains poorly constrained. The analysis also implies slightly higher masses for planets b, c, and f compared to suggestions by transit timing variation measurements. The work shows that the framework is capable of constraining important properties of planet formation models.

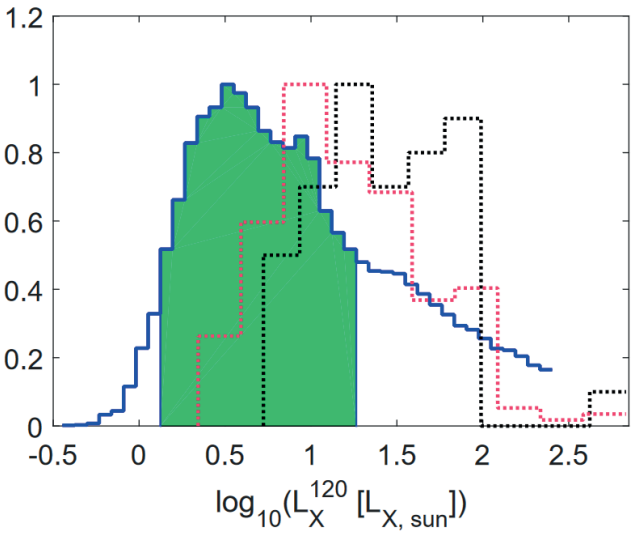

Posterior probability distribution for the X-ray luminosity of Kepler-11 at an age of 120 Myr (solid blue line; 68% confidence interval in green) in comparison to the distributions obtained for stars of similar spectral type in NGC 2516 (black dotted line; 48 stars) and for all detected stars in the same cluster (red dotted line; 239 stars).

TWO HOT SATURNS AND TWO JUPITERS, TWO OF THEM WITH METAL-RICH HOSTS

The SuperWASP exoplanet detection facility has led to the discovery of four transiting hot Saturns or Jupiters, WASP-147b, WASP-160Bb, WASP-164b, and WASP-165b. WASP-147b is a near Saturn-mass (M_P = 0.28 M_J) object with a radius of 1.11 R_J (see figure) orbiting a G4 star with a period of 4.6 d. WASP-160Bb has a mass and radius (M_p = 0.28 M_J, R_p = 1.09 R_J) nearly identical to WASP-147b, but is less irradiated, orbiting a metal-rich ([Fe/H] = 0.27) K0 star with a period of 3.8 d. WASP-160Bb is part of a near equal-mass visual binary with an on-sky separation of 28.5 arcsec. WASP-164b is a more massive (M_P = 2.13 M_J, R_p = 1.13 R_J) hot Jupiter, orbiting a G2 star on a close-in (P = 1.8 d), but tidally stable orbit. WASP-165b is a classical (M_p = 0.66 M_J, R_P = 1.26 R_J) hot Jupiter in a 3.5 d period orbit around a metal-rich ([Fe/H] = 0.33) star. The masses and radii of the newly detected planets are shown in the figure below. WASP-147b and WASP-160Bb are promising targets for atmospheric characterization through transmission spectroscopy, while WASP-164b represents a good target for emission spectroscopy.

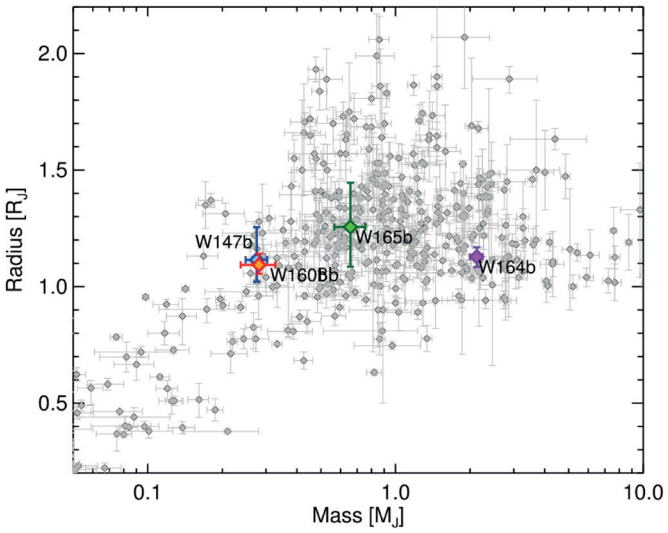

Planetary mass against planetary radius for known exoplanets. Only planets with well-measured masses and radii (relative uncertainties smaller than 50%) are shown. The newly-discovered objects are shown in color and labeled.

OPTICAL MODULATION PHASED WITH THE ORBIT OF SUPER-EARTH 55 Cnc e

55 Cnc e is a transiting super-Earth orbiting a solar-like star with an orbital period of just 17.7 hours. In 2011, the *MOST* satellite detected a quasi-sinusoidal flux modulation having the same period as the planetary orbit. The amplitude of this modulation was too large to be explained by a change in light reflected or emitted by the planet. The *MOST* telescope continued to observe 55 Cnc e for a few weeks per year over five years (from 2011 to 2015), covering 143 transits. Phase modulations similar to those seen in 2011 have been found in most of the subsequent years; however, the amplitude and phase of maximum light are seen to vary, from year to year, from 113 to 28 ppm and from 0.1 to 3.8 rad.

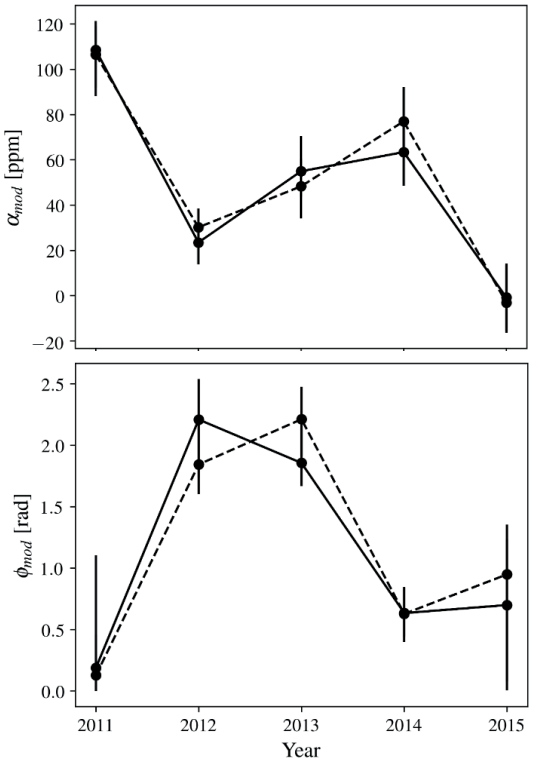

Evolution of the amplitudes (top) and orbital phases (bottom) parameters of the modulation in flux observed at the planet orbital period. The solid and dashed lines indicate the light curves detrended using two different methods.

The secondary eclipse is not detected, but the geometric albedo could nevertheless be constrained to <0.47 (2σ). While a single origin of the observed optical modulation could not be identified, the data are consistent with a few possible explanations. Those include star-planet interaction, such as coronal rains and spots rotating with the motion of the planet along its orbit, or the presence of a transiting circumstellar torus of dust. However, a detailed interpretation of these observations is limited by their photometric precision. Additional observations at optical wavelengths, e.g. with *CHEOPS*, could measure the variations at higher precision, contribute to uncovering the underlying physical processes, and measure or improve the upper limit on the albedo of the planet.

ANALYTIC THERMOCHEMICAL-EQUILIBRIUM ABUNDANCES

An analytic framework to obtain thermochemical-equilibrium abundances for H_2O, CO, CO_2, CH_4, C_2H_2, C_2H_4, HCN, NH_3, and N_2 for a system with known temperature, pressure, and elemental abundances has been previously developed. However, the implementation of that approach becomes numerically unstable under certain circumstances (e.g., C/O ≥ 1 atmospheres at low pressures). Building up on the already existing approach, the conditions that prompt inaccurate solutions have been identified, and a new framework to avoid them has been developed, providing a reliable implementation for arbitrary values of temperature (200 to 2000 K), pressure (10^{-8} to 10^{3} bar), and CNO abundances (10^{-3} to 10^{2} times solar elemental abundances), for hydrogen-dominated atmospheres.

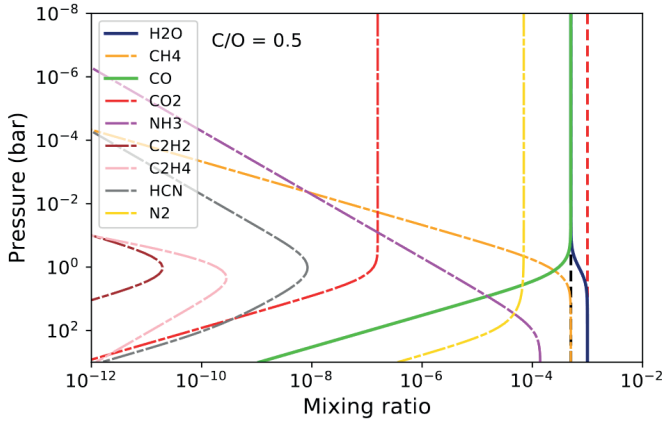

Thermochemical-equilibrium abundances for atmospheres with $N_C/N_O<1$. The atmosphere has a fixed temperature of 1200 K, $N_O=5\times10^{-4}$, and $N_N=7\times10^{-5}$. The black and red dashed vertical lines denote $2N_C$ and $2N_O$, which are related to the maximum values that carbon- and oxygen-bearing species can take, respectively.

The accuracy of the newly developed analytic framework is better than 10% for the more abundant species that have mixing fractions larger than 10^{-10}, whereas the accuracy is better than 50% for the less abundant species. Additionally, the equilibrium-abundance calculations of atomic and molecular hydrogen into the system have been added, and the physical limitations of this approach have been explored. Efficient and reliable tools, such as this one, are highly valuable for atmospheric Bayesian studies, which need to evaluate a large number of models. The new analytic framework has been implemented into the RATE Python open-source package.

HYDRODYNAMIC MODELLING OF IN-TRANSIT Lyα ABSORPTION OF GJ436b

The fully self-consistent 3D multi-fluid hydrodynamic model simulates the escaping upper atmosphere of warm Neptune GJ436b. It is driven by the stellar XUV radiation, gravitational forces, and interaction with the stellar wind, which is also simulated by the model. Calculations of in-transit absorption in Lyα in the simulated dynamical environment of GJ436b confirm that it is produced mostly by energetic neutral atoms outside the planetary Roche lobe, due to resonant thermal line broadening.

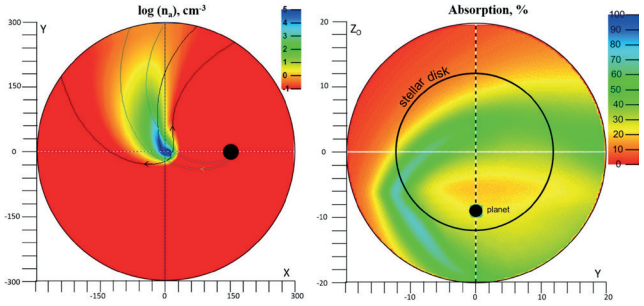

Distribution of atomic hydrogen density in the equatorial plane around GJ436b (left panel) and the line-of-sight absorption, averaged over the blue wing of the Lyα line, as seen by remote observer (right panel) calculated with typical SW parameters of GJ436.

The influence of radiation pressure was shown to be insignificant. By varying the model parameters it was possible to achieve reasonable agreement between the model predictions and observations (see figure below), e.g., in asymmetry of the absorbed Lyα line profile, transit depth (>70%) and early ingress. Some difference between the simulated and measured features can be explained by different stellar wind conditions during the measurement campaigns.

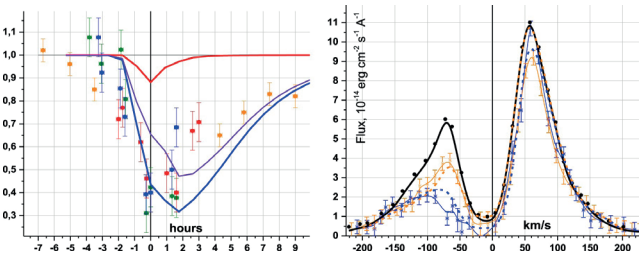

The simulated transit light curves of GJ436b in the blue ([-120; -40] km/s; blue line) and red ([30; 110] km/s; red line) wings of Lyα line (left panel) and the modeled Lyα line profiles at the mid-transit (t=0h; blue dashed) and post-transit (t=5h; orange dashed) phases (right panel). Observed data are shown by symbols with error bars. Black line depicts the out-of-transit case.

N_2/O_2-DOMINATED ATMOSPHERES ARE BIOMARKERS

Nitrogen is an essential element in the building blocks of life; hence, the geobiological nitrogen cycle is a fundamental factor in the long-term evolution of both Earth and Earth-like exoplanets. Since life-forms are the most efficient means for recycling deposited nitrogen back into the atmosphere at present, they sustain its surface partial pressure at high levels. Also, the simultaneous presence of significant N_2 and O_2 is chemically incompatible in an atmosphere over geological timescales. Thus, it is argued that an N_2-dominated atmosphere in combination with O_2 on Earth-like planets within circumstellar habitable zones can be considered as a geo-biosignature. Terrestrial planets with such atmospheres will have an operating tectonic regime connected with an aerobic biosphere, whereas other scenarios in most cases end up with a CO_2-dominated atmosphere.

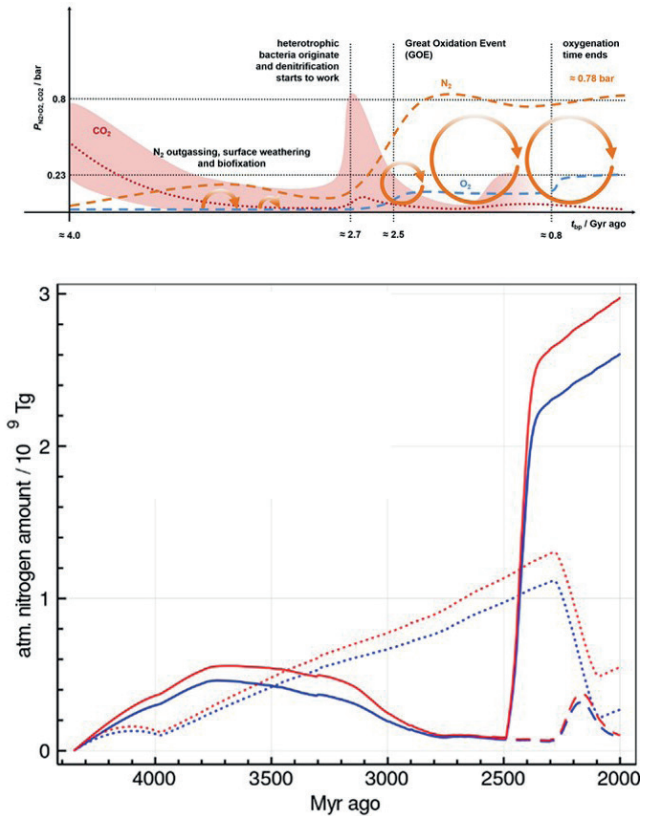

Upper panel: CO_2, N_2, O_2 surface partial pressure evolution on early Earth since about 4 Gyr ago. N_2 rose to the present values, when heterotrophic microorganisms responsible for denitrification led to the modern geobiological nitrogen cycle. Lower panel: Various atmospheric N_2 build up scenarios. Dotted lines: No life and solid lines – with life – scenarios, based on two different crust spreading outgassing models. The jump in N_2 release occurs due to denitrification caused by oxic life forms.

DUSTY PHENOMENA IN THE VICINITY OF GIANT EXOPLANETS

Photometric manifestations of dust around different kinds of exoplanets (mainly giants) were detected and investigated with a specially elaborated search and analysis technique applied to the long-cadence light curves recorded by NASA's *Kepler* space telescope. Using linear approximation of pre- and post-transit parts of the light curves of 118 Kepler objects of interest after their preliminary whitening and phase-folding, the corresponding flux gradients G1 and G2, were calculated before and after the transit border for two different time intervals: (a) from 0.03 to 0.16 days and (b) from 0.01 to 0.05 days, which characterize the distant and adjoining regions near the transiting object, respectively. The gradients G1 and G2 in the distant region clustered around zero, revealing the absence of signs of dusty obscuring matter (DOM) there. In the adjoining region, 17 cases of hot Jupiters showed significantly negative gradients G1, while G2 remained around zero (see upper panels). Visual analysis of individual cases also revealed the sporadic pre-transit decrease of flux, which systematically decreases G1 (see lower panels). This effect was reproduced with the models using a stochastic obscuring precursor ahead of the planet. Such phenomena may be caused by dusty atmospheric outflows, erosion and/or tidal decay of moonlets, or background circumstellar dust accumulated in electrostatic or magnetic traps in front of the mass-losing exoplanet.

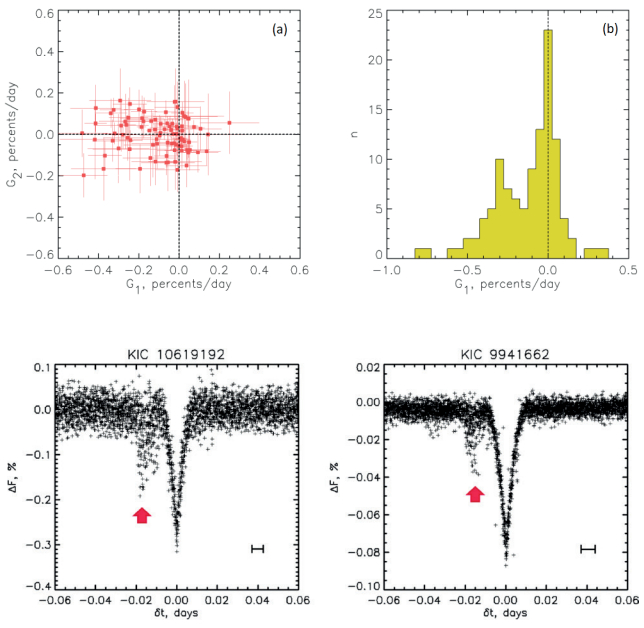

Upper panels: (a): Distribution of pre- (G1) and post- (G2) egress gradients in adjoining regions; (b): histogram of G1. Lower panels: Examples of DOM manifestations (arrowed) in the pre-ingress parts of folded and clipped light curves.

SATELLITE LASER RANGING

In addition to routinely tracking more than 150 targets, which are equipped with laser retro-reflectors, the Graz Satellite Laser Ranging (SLR) station is working on various projects. Recent highlights include first successful daylight space debris laser ranging, the design of a detection and laser package for ESA's new SLR station on Tenerife, and MHz laser ranging.

DAYLIGHT SPACE DEBRIS LASER RANGING

Orbit predictions of space debris objects based on Two Line Elements (TLE) are usually only accurate to within a few kilometers. Before the actual SLR search routine can be started space debris objects have to be centered within the field of view of the SLR station. The object has to be optically detected with an additional telescope using a larger field of view. So far space debris laser ranging was only possible close to the terminator zone, when it is already dark at the SLR station and the object in orbit is still illuminated by sunlight. The reflected sunlight can then be detected to correct inaccurate predictions centering the target in the field of view. To extend the observation times of space debris laser ranging to full daylight it is hence necessary to visualize such targets against the blue sky background. During daylight it was possible to observe stars up to magnitude 8.25 by using a CMOS camera together with a 780 nm edge filter to reduce the sky background noise.

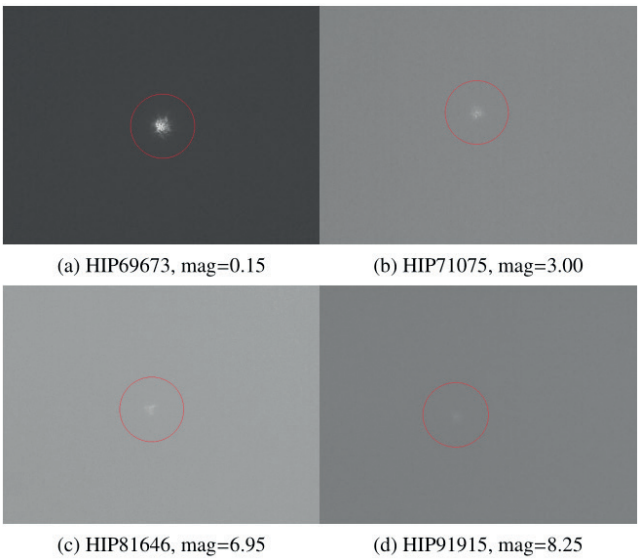

Daylight images of stars of the Hipparcos (HIP) catalog with magnitudes up to 8.25 observed at sun elevations between 10° and 18° with a 4.8 x 3.2 mm CMOS sensor (image cropped to 1.7 x 1.1 arc minutes).

In addition, more than 40 different rocket bodies were visualized (figure below). To be able to correct offsets to space debris objects a real-time image analysis software was developed. With respect to the predicted path the time bias and the azimuth/elevation pointing offsets are calculated. As Low Earth Orbit (LEO) satellite passes only last for a couple of minutes, directly after detection, the target is centered within the field of view and the SLR search routine is started.

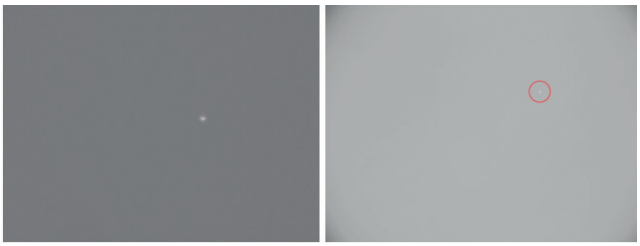

Sunlight reflections of two different rocket bodies imaged during daylight. SL-3 R/B (NORAD ID: 5118, left image) was captured within a sensor field of view of 3.4 x 2.3 arc minutes and SL-12 R/B (NORAD ID: 15772, right image, red circle) within 12.6 x 9.6 arc minutes.

Within four sessions six daylight space debris laser ranging passes were successfully observed (figure below, SL-16 rocket body) at sun elevations ranging from 2° to 39°. These first daylight space debris laser ranging results guide the way to significantly extend the potential observation times. Increased coverage will encourage the formation of an observation network similar to the International Laser Ranging Service (ILRS). Such a service could immediately react to improve the predictions in case of conjunctions or future removal missions.

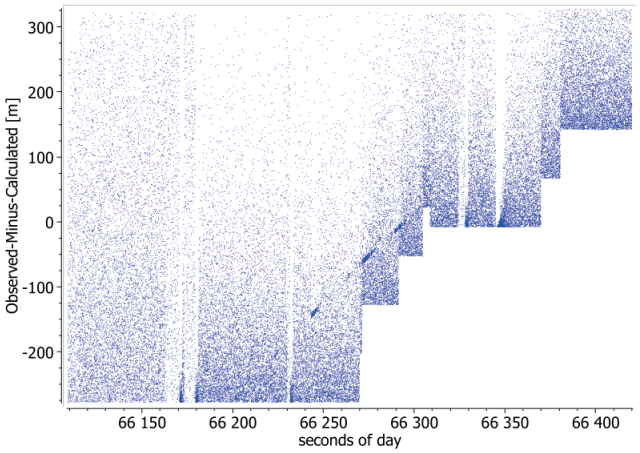

First successful daylight space debris laser ranging results to an SL-16 upper stage rocket body (NORAD ID: 23705). The figure shows the Observed-Minus-Calculated Residuals [m] vs. the seconds of day on 24 July 2019.

A NEW SLR STATION ON TENERIFE

In cooperation with an international consortium from Austria, Germany, Latvia and Switzerland the SLR station Graz is involved in the design and build-up of the first SLR station of the European Space Agency located on Teide on Tenerife. The station consists of an 80 cm Ritchey–Chrétien telescope on an altitude-azimuth mount with two Nasmyth and two folded-Cassegrain foci.

Graz is responsible for the design of the laser system, including laser, beam expansion optics and electronics for start pulse detection. The laser will be mounted directly on the telescope, avoiding any Coudé-path (multiple mirrors directing the laser beam from laboratory to the telescope). This new setup reduces the necessary alignment steps and is very cost effective and easy to handle. All optical components consist of commercial off-the-shelf parts.

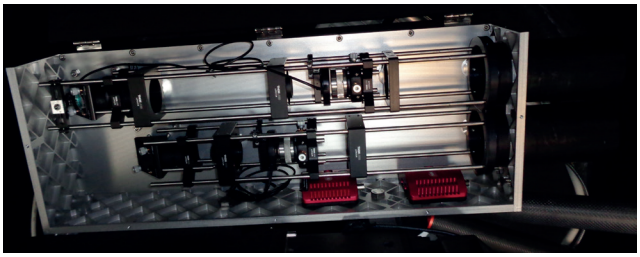

Final setup of the two color laser package with expansion optics to be installed on Tenerife in early 2020.

Furthermore, Graz develops the detection package consisting of two single photon avalanche diode detectors (SPAD, for green and infrared wavelength), an optical camera (for monitoring reflected sunlight from satellites), and an optional light curve detection system. The Astronomical Institute of Bern will install a highly sensitive optical space debris camera. The whole SLR system is built in a highly modular way, future extensions of the system include e.g. a space debris laser ranging package.

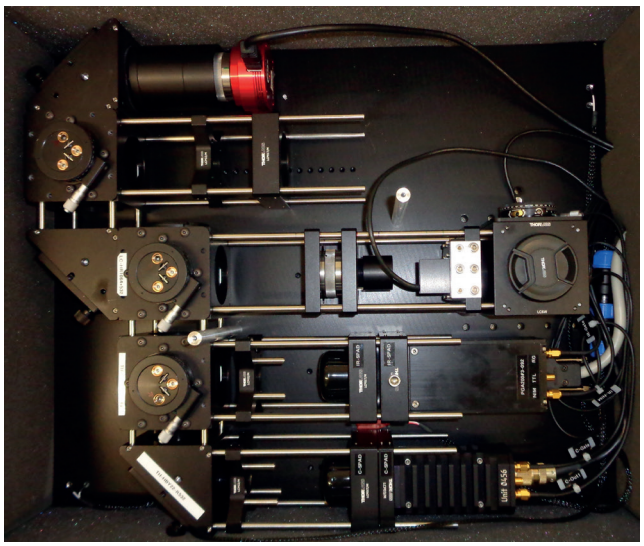

Final setup of the detection package including two SPAD detectors, an optical camera and an optional light curve detection system.

TOWARDS MHZ LASER RANGING

The SLR station Graz has been tracking cooperative targets routinely since 2 kHz SLR was developed in 2004. Ultra-high repetition (≥100 kHz) rate ranging is one of the most promising strategies for future SLR, and only few stations have already started such experiments. It delivers several benefits such as lower pulse energy, better statistical single-shot precision, higher resolution of target signature or shorter acquisition time for each normal point.

Between 8 and 10 August 2019, 500 kHz laser ranging was tested using a demo laser provided by IPG Photonics using a wavelength of 515 nm with pulse energies up to 50 µJ. Technical updates of hardware and software were developed such as a burst mode (see figure) for laser firing and range gate generation. To avoid the detection of backscatter the laser ranging is split into 4 phases: 1) laser transmission phase: laser firing until the first pulse is expected to arrive, 2) gap phase: waiting until atmospheric backscatter has arrived at the station, 3) receiving phase: detection of reflected SLR photons and 4) gap phase: time before the next laser burst is sent.

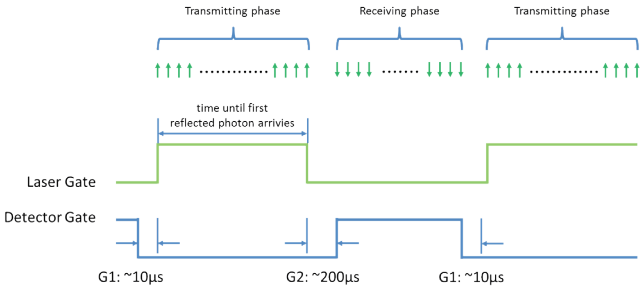

The burst mode for ultra-high repetition rate satellite laser ranging avoiding the detection of back scattered photons from the atmosphere.

Returns were successfully received up to a repetition rate of 500 kHz (limited by the event timer and the single photon detector). A return rate of approx. 2% was achieved for *Jason-2* (see figure), *Sentinel 3a* and *Sentinel 3b*. The accuracy and ranging performance of the laser, was verified ranging up to *GNSS* satellites with the same laser at 2 kHz using our routine setup.

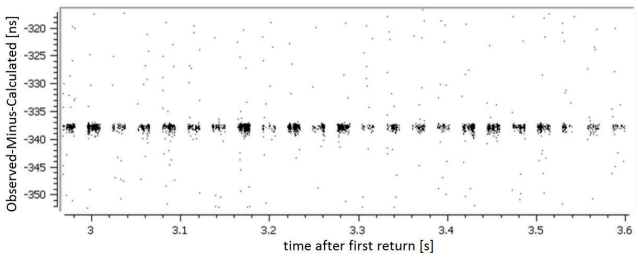

First 500 kHz laser ranging results to *Jason-2* (Observed-Minus-Calculated residuals [ns] vs time [s]). The laser and detector were operated in burst mode.

TECHNOLOGIES

NEW DEVELOPMENTS

One possible aspect to reduce costs of space exploration and hence allowing for more frequent missions is to reduce the spacecraft size and consequently the launch masses. Scientific instruments also have to decrease their resource requirements such as volume, mass, and power, but at the same time achieve at least the same performance as heritage instruments. Therefore, it is important that especially the instrument front-ends and readout units undergo miniaturization.

MAGNETOMETER FRONT-END ASIC

More than 15 years ago, IWF started to develop a miniaturized front-end electronics based on an Applications Specific Integrated Circuit (ASIC) for the readout of magnetic field sensors. The electronics chip is called Magnetometer Front-end ASIC (MFA).

The MFA flies successfully on NASA's *MMS* mission and on ESA's participation in the South Korean space weather satellite *GEO-KOMPSAT-2A (GK-2A)*. For both missions (*MMS* was launched in 2015 and *GK-2A* in 2018) and in total six flight magnetometers, the MFA shows superior functionality and competitive performance compared to magnetometers with discretely built electronics.

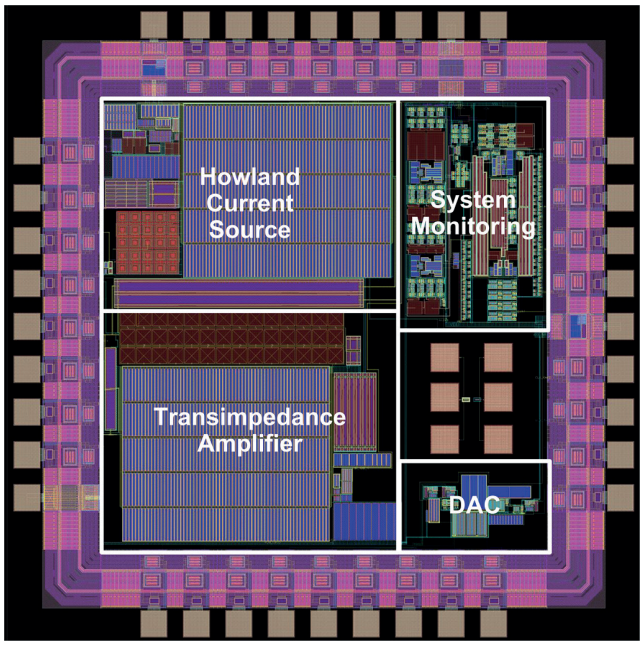

Layout of the second test chip implemented in 180 nm CMOS technology from United Microelectronics Corporation. The focus was on a high resolution feedback path with a signal-to-noise and distortion ratio >120 dB.

During the last two years, IWF and the Institute of Electronics of the Graz University of Technology have been working on a concept study for an improved version of the MFA in order to overcome dynamic range limitations and the fact that IWF is running out of qualified MFA chips. In 2019, the concept study was finished with the development, production and test of a second test chip (figure) as well as the elaboration of a detailed development and test plan for a space qualified, next generation MFA.

ASPOC NEXT GENERATION

For future science missions, active spacecraft potential control down to <10 V is crucial to be able to operate sensitive scientific payload. This does not only apply to large and medium-sized spacecraft, but also to micro- and nano-spacecraft, such as CubeSats. IWF (hardware) together with FOTEC (emitter) started a two-year technology study, with the goal to develop a miniaturized version (50% power, 40% mass) of the *ASPOC* instruments built for NASA's *MMS* mission, which operate flawlessly for more than five years.

PROSPECT PERMITTIVITY SENSOR

A sensor prototype was developed for ESA's Lunar Prospect. The permittivity sensor can determine the electrical permittivity (ε_r) of materials in contact with the sensor electrode via a comparison of the electrode current measured for air/vacuum and for contact with the material of interest. The sensor is designed for the expected Luna-27 environment (dry, cold Lunar surface materials).

The whole electrode and electronic package was required to fit within the diameter of the sampling drill developed by ESA. Thus, a major constraint of the development was the limited space available and a thermally uncontrolled cold environment. The sensor electronics is located 60 cm upwards but as well inside the drill tube. The applied electrode signal is a square wave, which contains multiple frequency components. The acquisition and analysis of the sensor output signal therefore allows a concurrent multi-frequency measurement. A fixed frequency square wave of 1.6 Hz is generated and sent into the adjacent soil via a small electrode embedded in the hull of the drill stem. The current return path is via the metallic tube of the drill itself.

A particular challenge was the decision to use 3D printed parts for the electrode and PCB (printed circuit board) holder. This decision helped to speed up the manufacturing and implementing design change of the mechanical parts. At the same time, integrating the design constraints for printed PEEK parts required different design approaches in comparison to classical mechanical production.

INFRASTRUCTURE

Instruments aboard spacecraft are exposed to harsh environments, e.g., vacuum, large temperature ranges, radiation, and high mechanical loads during launch. Furthermore, these instruments are expected to be highly reliable, providing full functionality over the entire mission time, which could last for more than a decade.

IWF owns several test facilities and special infrastructure for the production of flight hardware. A high-performance computer helps the scientists to cope with the enormous data, which have to be analyzed for space missions.

FLIGHT HARDWARE PRODUCTION

Flight hardware is assembled and tested in the institute's ISO 7 *Clean Room*. It has a total area of 30 m^2 containing a 5 m^2 quasi ISO 6 compartment. For clean storage or smaller assembly work and testing a HEPA-filtered air (HEPA = High Efficiency Particulate Air) laminar flow Clean Bench is available.

The *Vapor Phase Soldering (VPS) Machine* provides a flexible, simple and most reliable soldering method ideally suited for all types of surface mounted device (SMD) components. This VPS machine together with the hand soldering stations, a *Fluid Dispensing System*, which allows a precise dosing of solder pastes on PCBs, and an *Infrared Soldering Machine* mainly used for rework, allows the certified operators to assemble ESA qualified PCBs.

MAGNETOMETER CALIBRATION

At the institute, IWF operates several *multi-layer magnetic shieldings*, a wooden *3D Helmholtz coil system* and a special *temperature test facility* for all basic magnetometer performance and calibration tests as well as for the evaluation of the magnetic moments of satellite subsystems. Furthermore, a *3D Merritt coil system* (photo below) was installed at the Conrad Observatory in cooperation with the Zentralanstalt für Meteorologie und Geodynamik (ZAMG). It enables a precise calibration of magnetic sensors in a magnetically very clean environment.

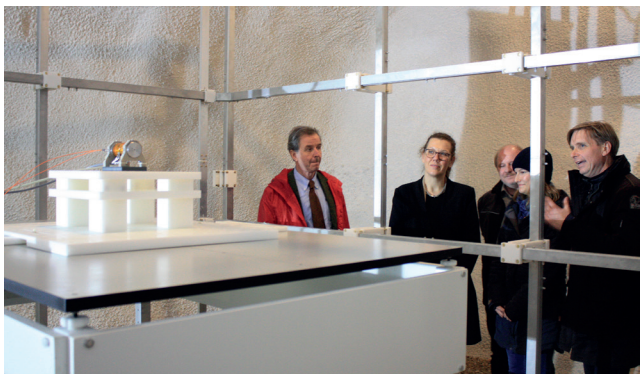

IWF presented the *JUICE* sensor to Federal Minister Iris Rauskala during a media day at the ZAMG Conrad Observatory (© ZAMG).

TEST FACILITIES

IWF hosts three vacuum chambers. The *Small Vacuum Chamber* (160 mm diameter, 300 mm length) is used for small electronic components or PCBs. The *Medium Vacuum Chamber* (700 mm diameter, 850 mm length) contains a target manipulator with two axes and an ion beam source. This chamber mainly serves for functional tests of the *PICAM* Flight Spare Model. The *Large Vacuum Chamber* (650 mm diameter, 1650 mm length) features a target manipulator for computer-controlled rotation of the target around three mutually independent perpendicular axes, a permalloy layer for magnetic shielding, and a heater around the circumference for baking of structures and components to outgas volatile products and unwanted contaminations.

Two *Temperature Test Chambers* with a capacity of 190 l and 37 l, respectively, allow to check the temperature resistance of electronic components and assemblies from down to -70 °C up to +180 °C. Both are equipped with a 32-bit control and communication system.

The *Thermal Vacuum Chamber* combines the capabilities of vacuum and temperature test chambers. At a pressure level of 10^{-6} mbar thermal cycling in a temperature range between -90 °C and +140 °C can be executed. Thermal cycling tests are mandatory for the qualification and acceptance of flight hardware.

The 40x40 mm *Surface Laboratory Chamber* supports surface science research between -90 °C and +50 °C.

The *Sample Chamber* contains an 8µ particle filter and allows measurements of grain sample electrical permittivity. The additional *Small Sample Chamber* can be used to derive the gas diffusion coefficient in porous samples.

The *Penetrometry Test Stand* is designed to measure mechanical soil properties, like bearing strength. The UV exposure facility is capable to produce radiation between 200-400 nm (UV-A, UV-B, UV-C).

HIGH-PERFORMANCE COMPUTER

With the LEO computing cluster, IWF hosts a small high-performance computer for diverse kinds of simulations, ranging from fundamental plasma physics, electron dynamics, magneto-hydrodynamical models, and magnetic reconnection in the Earth's magnetosphere to the atmospheric evolution on diverse planets. On top, the system provides processing power and data storage for current and completed missions. The current storage capacity reaches 600 TB on regular hard disks and 64 TB on especially durable and fast solid state devices. The working memory totals to 8 TB of RAM.

For further information on the IWF infrastructure refer to the dedicated submenu on iwf.oeaw.ac.at/en/institute/infrastructure.

OUTREACH

PUBLIC OUTREACH

IWF is actively engaged in science education and public outreach. In 2019 the emphasis was on the 50th anniversary of the moon landing and the launch of *CHEOPS*.

The PR year was opened on 16 February by the "Weltraumball", organized by the Austrian Space Forum (ÖWF), where IWF presented a small exhibition on Mercury/*BepiColombo* and exoplanets/*CHEOPS*.

At the IMST Networking Day on 28 February, Werner Magnes gave a presentation at Pädagogische Hochschule Steiermark. IMST (Innovationen Machen Schulen Top) supports small MIST projects in Styrian schools.

On 6-7 June, the Fifteen Seconds Festival took place in Graz. IWF presented the *CHEOPS* mission at this conference with 200 international speakers and 6000 visitors from German speaking countries (photo below).

On 25 June, the exhibition on "50 Years Moon Landing" at the Technical Museum in Vienna opened. ESA Director Günther Hasinger talked about the new insights in space research and IWF Director Wolfgang Baumjohann was part of a panel discussion about the Austrian contributions.

At the "100 Jahre URSI" symposium, organized by the ÖAW Commission for Astronomy at IWF, Bruno Besser and Martin Volwerk discussed Austria's radio science heritage and comet tail physics.

In July, IWF was invited for the first time to Kinderuni Wien. Bruno Besser informed the 7-12 years old "university students" about our solar system and Günter Kargl planned a satellite mission with them.

Ars Electronica Linz also dedicated a weekend to the moon landing anniversary, during which Bruno Besser talked about Austria's history in space.

At the Summer School on "Natural Space Risks", held at Paris Observatory from 26-31 August, Christoph Lhotka referred about "Space weathering effects on space dust dynamics".

On 28 August, Herbert Lichtenegger, Ferdinand Plaschke, Manfred Steller, and Martin Volwerk talked about Mercury, the Earth's magnetosphere, exoplanets, and comets to the ten-year old participants of the space camp during the summer school of WIKU BRG Graz.

CHEOPS booth and IWF team at the Fifteen Seconds Festival.

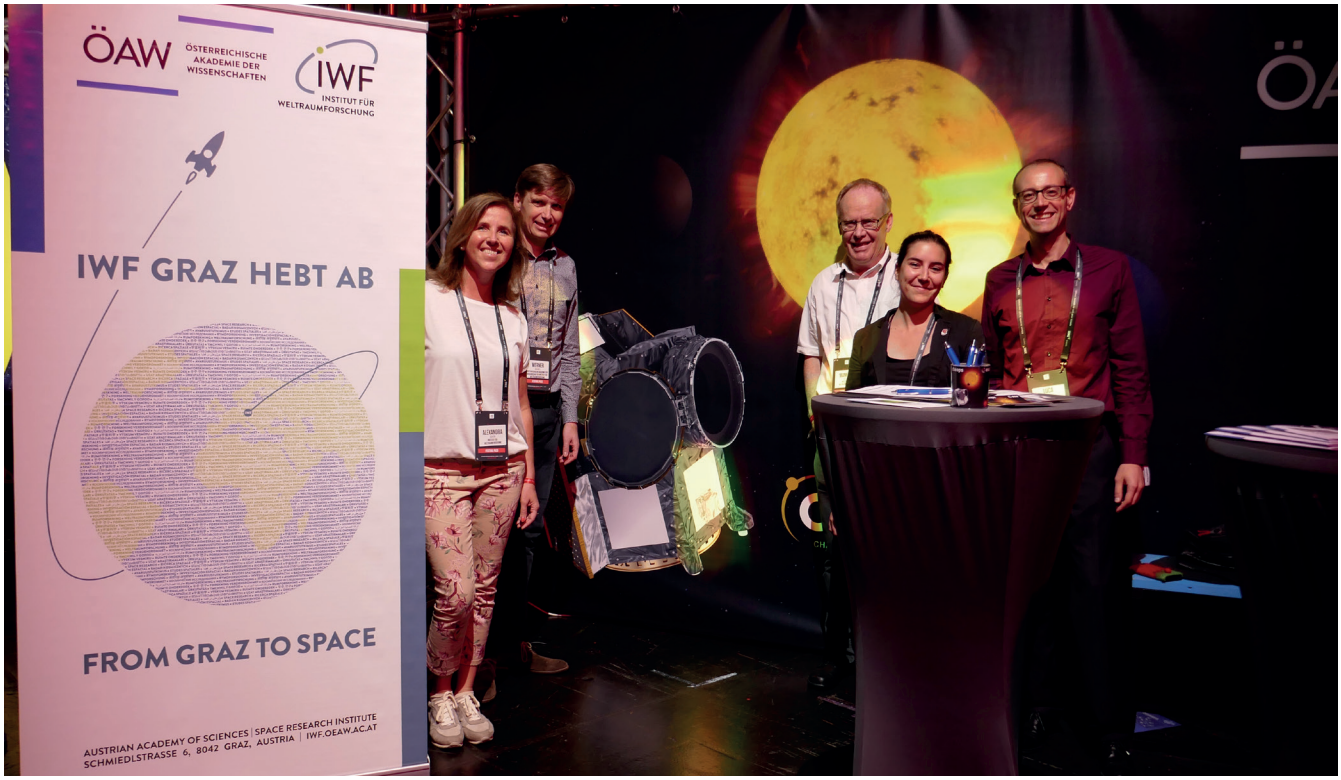

During summer time, five high-school students performed an internship at IWF under the "Talente-Praktika" program of FFG. They worked on *CSES* magnetic field measurements, remote sensing of Earth's ionosphere, processing of weather data, graphical interface for *PICAM*, and the bow shock of Venus and Mars. In the framework of the "FEMtech" program of FFG, five female students from the University of Graz and Graz University of Technology worked at IWF on space weather, magnetotail dynamics, CUTE, Graz climate, and heliospheric dust.

On 27 September, IWF presented ESA's *CHEOPS* mission during the European Researchers' Night (ERN), a mega event that takes place every year simultaneously in several hundred cities all over Europe and beyond (right photo).

BRG Kepler invited IWF to participate in the "Long Museum Night" on 5 October. Luca Fossati presented IWF's current space missions with emphasis on *CHEOPS*.

Luca Fossati presented this year's Nobel laureates in Physics during a dedicated colloquium at the University of Graz on 28 October.

On 6 November, ÖAW invited IWF to the academy's Comics Day, in which the science comics laureates and their work were presented to 8-12 year olds. IWF entertained 200 school kids with a special program on exoplanets. In Volume 1 of the comics series "Akademics" researchers from IWF and other ÖAW institutes answer "1000 Fragen rund um eine Kartoffel" (www.oeaw.ac.at/akademics/kartoffel-im-weltall#comic).

Hundreds of rockets were cut, glued and then launched during ERN 2019 at the University of Applied Arts Vienna (© PRIA/Simon Kupferschmied).

Countdown for *CHEOPS'* "test launch" during the Comics Day held at the ÖAW headquarters (© ÖAW).

The Austrian Science Fund FWF and "Wiener Zeitung" organized the discussion evening "Am Puls No. 67" on 4 December. Günter Kargl and "austronaut" Franz Viehböck talked about how the settlement of other planets affects our society.

Günter Kargl (left) and Franz Viehböck during the FWF panel discussion (© FWF/Christine Mies).

On 17 December, IWF/ÖAW and FFG organized a launch party for ESA's *CHEOPS* mission in Graz and Vienna. Unfortunately, the 300 guests, including the Federal Ministers Andreas Reichhardt and Iris Rauskala, could not follow the launch live, because it was delayed by one day. Nevertheless, the presentations and guided tours through the laboratory still continued.

One of the many laboratory visits, which IWF offers to young future researchers throughout the year.

Throughout the year, Bruno Besser, Philippe Bourdin, Luca Fossati, and Wolfgang Voller participated in three URANIA lecture series, honoring 50 years of moon landing and 30 years of astronomy (at URANIA Graz).

Topics discussed in the space blog of the Austrian newspaper "Der Standard" were the launch of *BepiColombo*, space debris, and antenna calibration for *JUICE*.

Audio science is provided in the ÖAW podcasts MAKRO MIKRO. In episode #6, Luca Fossati discussed extraterrestrial life (soundcloud.com/makro-mikro).

AWARDS & RECOGNITION

ÖAW elected Rumi Nakamura as a Corresponding Member in Austria of the Division of Mathematics and the Natural Sciences. She was also elected a member of the Academia Europaea.

Wolfgang Baumjohann received the "Kardinal-Innitzer-Würdigungspreis" for Natural Sciences/Medicine.

The outstanding achievements of former IWF director Hans Sünkel were acknowledged with the award of a Ring of Honor by the City of Graz.

Mayor Siegfried Nagl (left) and Hans Sünkel during the award ceremony in the Graz town hall (© Fischer - Stadt Graz).

Bruno Besser was awarded with the Werner Welzig Prize of ÖAW, honoring his contribution to the internal cohesion and public prestige of the academy. An interdisciplinary Austrian jury selected Monika Lendl as FEMtech (women in research and technology) researcher of February. Last but not least, AGU selected Takuma Nakamura as an "Outstanding Reviewer".

LECTURING AND MENTORING

In summer 2019 and in winter term 2019/2020 IWF members gave lectures at the University of Graz, Graz University of Technology, University of Vienna, TU Braunschweig, FH Joanneum, and FH Wiener Neustadt.

In the framework of the ÖAW mentoring system, organized by the Working Group on Non-Discrimination of ÖAW, Martin Volwerk served as mentor.

MEETINGS

From 15-18 April, IWF organized the international conference "PLATO Week #8" at TU Graz with approximately 100 participants.

Wolfgang Baumjohann served as Vice Director and chair of the Program Committee of the Summer School Alpbach, which took place from 16 to 25 July and was dedicated to "Geophysics from Space Using Micro- or Nano-Satellite Constellations". Every year, 60 students and about 25 lecturers and tutors from ESA's member states are invited to this meeting.

From 16-20 September, IWF organized a Magnetometer Workshop in Stubenberg am See, Styria, with 45 participants (photo below).

In the last week of September, IWF hosted the *JUICE/RPWI* team meeting.

On 10 and 11 October, the *CUTE* Science Team Meeting was organized at IWF, bringing about a dozen scientists together.

In addition, M.Y. Boudjada, M. Delva, N.K. Dwivedi, L. Fossati, M.L. Khodachenko, W. Magnes, R. Nakamura, E. Panov, F. Plaschke, M. Steller, and M. Volwerk were members of scientific program and/or organizing committees at six international conferences and/or workshops.

THESES

Besides lecturing, members of the institute are supervising Bachelor, Diploma, Master and Doctoral Theses. In 2019, the following supervised theses have been completed:

Ellmeier, M.: Evaluation of the Optical Path and the Performance of the Coupled Dark State Magnetometer, Doctoral Thesis, Technische Universität Graz, 178 pages, 2019.

Schirninger, C.: Magnetic Field Investigations of Volcanic and Seismic Phenomena with the China Seismo-Electromagnetic Satellite (CSES), Bachelor Thesis, Technische Universität Graz, 48 pages, 2019.

Wellenzohn, S.: Energy Dispersion in the PSBL Flows during Substorms, Diploma Thesis, Universität Graz, 58 pages, 2019

Participants of the Magnetometer Workshop in Stubenberg am See.

PUBLICATIONS

REFEREED ARTICLES

Angelopoulos, V., P. Cruce, A. Drozdov, E.W. Grimes, N. Hatzigeorgiu, D.A. King, D. Larson, J.W. Lewis, J.M. McTiernan, D.A. Roberts, C.L. Russell, T. Hori, Y. Kasahara, A. Kumamoto, A. Matsuoka, Y. Miyashita, Y. Miyoshi, I. Shinohara, M. Teramoto, J.B. Faden, A.J. Halford, M. McCarthy, R.M. Millan, J.G. Sample, D.M. Smith, L.A. Woodger, A. Masson, A.A. Narock, K. Asamura, T.F. Chang, C.-Y. Chiang, Y. Kazama, K. Keika, S. Matsuda, T. Segawa, K. Seki, M. Shoji, S.W.Y. Tam, N. Umemura, B.-J. Wang, S.-Y. Wang, R. Redmon, J.V. Rodriguez, H.J. Singer, J. Vandegriff, S. Abe, M. Nose, A. Shinbori, Y.-M. Tanaka, S. UeNo, L. Andersson, P. Dunn, C. Fowler, J.S. Halekas, T. Hara, Y. Harada, C.O. Lee, R. Lillis, D.L. Mitchel, M.R. Argall, K. Bromund, J.L. Burch, I.J. Cohen, M. Galloy, B. Giles, A.N. Jaynes, O. Le Contel, M. Oka, T.D. Phan, B.M. Walsh, J. Westlake, F.D. Wilder, S.D. Bale, R. Livi, M. Pulupa, P. Whittlesey, A. DeWolfe, B. Harter, E. Lucas, U. Auster, J.W. Bonnel, C.M. Cully, E. Donovan, R.E. Ergun, H.U. Frey, B. Jackel, A. Keiling, H. Korth, J.P. McFadden, Y. Nishimura, F. Plaschke, P. Robert, D.L. Turner, J.M. Weygand, R.M. Candey, R.C. Johnson, T. Kovalick, M.H. Liu, R.E. McGuire, A. Breneman, K. Kersten, P. Schroeder: The Space Physics Environment Data Analysis System (SPEDAS), *Space Sci. Rev.*, **215**, 9, 2019.

Archer, M.O., H. Hietala, M.D. Hartinger, F. Plaschke, V. Angelopoulos: Direct observations of a surface eigenmode of the dayside magnetopause, *Nat. Comm.*, **10**, 615, 2019.

Arkhypov, O.V., M.L. Khodachenko, A. Hanslmeier: Dusty phenomena in the vicinity of giant exoplanets, *Astron. Astrophys.*, **631**, A152, 2019.

Bader, A., G. Stenberg Wieser, M. André, M. Wieser, Y. Futaana, M. Persson, H. Nilsson, T.L. Zhang: Proton temperature anisotropies in the plasma environment of Venus, *J. Geophys. Res.*, **124**, 3312-3330, 2019.

Barkaoui, K., A. Burdanov, C. Hellier, M. Gillon, B. Smalley, P.F.L. Maxted, M. Lendl, A.H.M.J. Triaud, D.R. Anderson, J. McCormac, E. Jehin, Y. Almleaky, D.J. Armstrong, Z. Benkhaldoun, F. Bouchy, D.J.A. Brown, A.C. Cameron, A. Daassou, L. Delrez, E. Ducrot, E. Foxell, C. Murray, L.D. Nielsen, F. Pepe, D. Pollacco, F.J. Pozuelos, D. Queloz, D. Segransan, S. Udry, S. Thompson, R.G. West: Discovery of three new transiting Hot Jupiters: WASP-161 b, WASP-163 b, and WASP-170 b, *Astron. J.*, **157**, 43, 2019.

Barnes, D., J.A. Davies, R.A. Harrison, J.P. Byrne, C.H. Perry, V. Bothmer, J.P. Eastwood, P.T. Gallagher, E.K.J. Kilpua, C. Möstl, L. Rodriguez, A.P. Rouillard, D. Odstrcil: CMEs in the heliosphere: II. A statistical analysis of the kinematic properties derived from single-spacecraft geometrical modelling techniques applied to CMEs detected in the heliosphere from 2007 to 2017 by STEREO/HI-1, *Solar Phys.*, **294**, 57, 2019.

Barragán, O., S. Aigrain, D. Kubyshkina, D. Gandolfi, J. Livingston, M.C.V. Fridlund, L. Fossati, J. Korth, H. Parviainen, L. Malavolta, E. Palle, H.J. Deeg, G. Nowak, V.M. Rajpaul, N. Zicher, G. Antoniciello, N. Narita, S. Albrecht, L.R. Bedin, J. Cabrera, W.D. Cochran, J. de Leon, Ph. Eigmüller, A. Fukui, V. Granata, S. Grziwa, E. Guenther, A.P. Hatzes, N. Kusakabe, D.W. Latham, M. Libralato, R. Luque, P. Monta nés-Rodríguez, F. Murgas, D. Nardiello, I. Pagano, G. Piotto, C.M. Persson, S. Redfield, M. Tamura: Radial velocity confirmation of K2-100b: A young, highly irradiated, and low density transiting hot Neptune, *MNRAS*, **490**, 698–708, 2019.

Barrie, A.C., F. Cipriani, C.P. Escoubet, S. Toledo-Redondo, R. Nakamura, K. Torkar, Z. Sternovsky, S. Elkington, D. Gershman, B. Giles, C. Schiff: Characterizing spacecraft potential effects on measured particle trajectories, *Phys. Plasmas*, **26**, 103504, 2019.

Bell, T.J., M. Zhang, P.E. Cubillos, L. Dang, L. Fossati, K.O. Todorov, N.B. Cowan, D. Deming, R.T. Zellem, K.B. Stevenson, I.J.M. Crossfield, I. Dobbs-Dixon, J.J. Fortney, H.A. Knutson, M.R. Line: Mass loss from the exoplanet WASP-12b inferred from Spitzer phase curves, *MNRAS*, **489**, 1995-2013, 2019.

Berezutsky, A.G., I.F. Shaikhislamov, I.B. Miroshnichenko, M.S. Rumenskikh, M.L. Khodachenko: Interaction of the expanding atmosphere with the stellar wind around Gliese 436b, *Solar Syst. Res.* , **53**, 138-145, 2019.

Borsa, F., M. Rainer, A.S. Bonomo, D. Barbato, L. Fossati, L. Malavolta, V. Nascimbeni, A.F. Lanza, M. Esposito, L. Affer, G. Andreuzzi, S. Benatti, K. Biazzo, A. Bignamini, M. Brogi, I. Carleo, R. Claudi, R. Cosentino, E. Covino, M. Damasso, S. Desidera, A. Garrido Rubio, P. Giacobbe, E. González-Álvarez, A. Harutyunyan, C. Knapic, G. Leto, R. Ligi, A. Maggio, J. Maldonado, L. Mancini, A.F. M. Fiorenzano, S. Masiero, G. Micela, E. Molinari, I. Pagano, M. Pedani, G. Piotto, L. Pino, E. Poretti, G. Scandariato, R. Smareglia, A. Sozzetti: The GAPS Programme with HARPS-N at TNG. XIX. Atmospheric Rossiter-McLaughlin effect and improved parameters of KELT-9b, *Astron. Astrophys.*, **631**, A34, 2019.

Breuillard, H., P. Henri, L. Bucciantini, M. Volwerk, T. Karlsson, A. Eriksson, F. Johansson, E. Odelstad, I. Richter, C. Goetz, X. Vallières, R. Hajra: Properties of the singing comet waves in the 67P/Churyumov-Gerasimenko plasma environment as observed by the Rosetta mission, *Astron. Astrophys.*, **830**, A39, 2019.

Chai, L.H., W.X. Wan, Y. Wei, T.-L. Zhang, W. Exner, M. Fraenz, E. Dubinin, M. Feyerabend, U. Motschmann, Y.J. Ma, J.S. Halekas, Y. Li, Z.J. Rong, J. Zhong: The induced global looping magnetic field on Mars, *Astrophys. J. Lett.*, **871**, L27, 2019.

Chang, Q., X. Xu, Q. Xu, J. Zhong, J. Xu, J. Wang, T.L. Zhang: Multiple-point modeling the Parker spiral configuration of the solar wind magnetic field at the solar maximum of solar cycle 24, *Astrophys. J.*, **884**, 102, 2019.

Chargeishvili, B.B., D.A. Maghradze, D.R. Japaridze, N.B. Oghrapishvili, T.G. Mdzinarishvili, K.B. Chargeishvili, B.M. Shergelashvili: Variation of coronal holes latitudinal distribution: Correction of limb brightening of EUV coronal images, *Adv. Space Res.*, **64**, 491-503, 2019.

Chen, Y., T.-Long Zhang, M. Wu, G. Wang, D. Schmid, W. Baumjohann, R. Nakamura, C.T. Russell, B.J. Giles, J.L. Burch: Small spatial-scale field-aligned currents in the plasma sheet boundary layer surveyed by Magnetosphere Multiscale Spacecraft, *J. Geophys. Res.*, **124**, 9976–9985, 2019.

Chen, Y.Q., M. Wu G. Wang, D. Schmid, T.L. Zhang, R. Nakamura, W. Baumjohann, J.L. Burch, B.J. Giles, C.T. Russell: Carriers of the field-aligned currents in the plasma sheet boundary layer: An MMS multicase study, *J. Geophys. Res.*, **124**, 2873-2886, 2019.

Cherenkov, A.A., I.F. Shaikhislamov, D.V. Bisikalo, V.I. Shematovich, L. Fossati, C. Möstl: The influence of superflares of host stars on the dynamics of the envelopes of Hot Jupiters, *Astron. Rep.*, **63**, 94-106, 2019.

Comisel, H., Y. Narita, U. Motschmann: Multi-channel coupling of decay instability in three-dimensional low-beta plasma, *Ann. Geophys.*, **37**, 835-842, 2019.

Cozzani, G., A. Retinò, F. Califano, A. Alexandrova, O. Le Contel, Y. Khotyaintsev, A. Vaivads, H.S. Fu, F. Catapano, H. Breuillard, N. Ahmadi, P.-A. Lindqvist, R.E. Ergun, R.B. Torbert, B.L. Giles, C.T. Russell, R. Nakamura, S. Fuselier, B.H. Mauk, T. Moore, J.L. Burch: In situ spacecraft observations of a structured electron diffusion region during magnetopause reconnection, *Phys. Rev. E*, **99**, 043204, 2019.

Cubillos, P.E., J. Blecic, I. Dobbs-Dixon: Toward more reliable analytic thermochemical-equilibrium abundances, *Astrophys. J.*, **872**, 111, 2019.

De Spiegeleer, A., M. Hamrin, H. Gunell, M. Volwerk, L. Andersson, T. Karlsson, T. Pitkänen, C.G. Mouikis, H. Nilsson, L.M. Kistler: Oscillatory flows in the magnetotail plasma sheet: Cluster observations of the distribution function, *J. Geophys. Res.*, **124**, 2736-2754, 2019.

De Spiegeleer, A., M. Hamrin, M. Volwerk, T. Karlsson, H. Gunell, G.S. Chong, T. Pitkänen, H. Nilsson: Oxygen ion flow reversals in Earth's magnetotail: A Cluster statistical study, *J. Geophys. Res.*, **124**, 8928-8942, 2019.

Dehant, V., V. Debaille, V. Dobos, F. Gaillard, C. Gillmann, S. Goderis, J.L. Grenfell, D. Höning, E.J. Javaux, Ö. Karatekin, A. Morbidelli, L. Noack, H. Rauer, M. Scherf, T. Spohn, P. Tackley, T. Van Hoolst, K. Wünnemann: Geoscience for understanding habitability in the solar system and beyond, *Space Sci. Rev.*, **215**, 42, 2019.

Dididze, G., B.M. Shergelashvili, V.N. Melnik, V.V. Dorovskyy, A.I. Brazhenko, S. Poedts, T.V. Zaqarashvili, M.L. Khodachenko: Comparative analysis of solar radio bursts before and during CME propagation, *Astron. Astrophys.*, **625**, A63, 2019.

Divin, A., V.S. Semenov, I. Zaitsev, D. Korovinskiy, J. Deca, G. Lapenta, V. Olshevsky, S. Markidis: Inner and outer electron diffusion region of antiparallel collisionless reconnection: Density dependence, *Phys. Plasmas*, **26**, 102305, 2019.

Dragomir, D., J. Teske, M.N. Günther, D. Ségransan, J.A. Burt, C.X. Huang, A. Vanderburg, E. Matthews, X. Dumusque, K.G. Stassun, J. Pepper, G.R. Ricker, R. Vanderspek, D.W. Latham, S. Seager, J.N. Winn, J.M. Jenkins, T. Beatty, F. Bouchy, T.M. Brown, R.P. Butler, D.R. Ciardi, J.D. Crane, J.D. Eastman, L. Fossati, J. Francis, B.J. Fulton, B.S. Gaudi, R.F. Goeke, D. James, T.C. Klaus, R.B. Kuhn, C. Lovis, M.B. Lund, S. McDermott, M. Paegert, F. Pepe, J.E. Rodriguez, L. Sha, S.A. Shectman, A. Shporer, R.J. Siverd, A. Garcia Soto, D.J. Stevens, J.D. Twicken, S. Udry, S. Villanueva, Jr., S.X. Wang, B. Wohler, X. Yao, Z. Zhan: TESS delivers its first Earth-sized planet and a warm sub-Neptune, *Astrophys. J. Lett.*, **875**, L7, 2019.

Dumbović, M., J. Guo, M. Temmer, M. Leila Mays, A. Veronig, S.G. Heinemann, K. Dissauer, S. Hofmeister, J. Halekas, C. Möstl, T. Amerstorfer, J. Hinterreiter, S. Banjac, K. Herbst, Y. Wang, L. Holzknecht, M. Leitner, R.F. Wimmer-Schweingruber: Unusual plasma and particle signatures at Mars and STEREO-A related to CME-CME interaction, *Astrophys. J.*, **880**, 18, 2019.

Dwivedi, N.K., M.L. Khodachenko, I.F. Shaikhislamov, L. Fossati, H. Lammer, Y. Sasunov, A.G. Berezutskiy, I.B. Miroshnichenko, K.G. Kislyakova, C.P. Johnstone, M. Güdel: Modelling atmospheric escape and Mg II near-ultraviolet absorption of the highly irradiated hot Jupiter WASP-12b, *MNRAS*, **487**, 4208-4220, 2019.

Dwivedi, N.K., S. Kumar, P. Kovacs, E. Yordanova, M. Echim, R.P. Sharma, M.L. Khodachenko, Y. Sasunov: Implication of kinetic Alfvén waves to magnetic field turbulence spectra: Earth's magnetosheath, *Astrophys. Space Sci.*, **364**, 101, 2019.

Echim, M.M., H. Lamy, J. De Keyser, R. Maggiolo, H. Gunell, C.L.S. Wedlund: A method to estimate the physical properties of magnetospheric generators from observations of quiet discrete auroral arcs, *J. Geophys. Res.*, **124**, 10283–10293, 2019.

Ergun, R.E., S. Hoilijoki, N. Ahmadi, S.J. Schwartz, F.D. Wilder, J.F. Drake, M. Hesse, M.A. Shay, H. Ji, M. Yamada, D.B. Graham, P.A. Cassak, M. Swisdak, J.L. Burch, R.B. Torbert, J.C. Holmes, J.E. Stawarz, K.A. Goodrich, S. Eriksson, R.J. Strangeway, O. LeContel: Magnetic reconnection in three dimensions: Modeling and analysis of electromagnetic drift waves in the adjacent current sheet, *J. Geophys. Res.*, **124**, 10085-10103, 2019.

Ergun, R.E., S. Hoilijoki, N. Ahmadi, S.J. Schwartz, F.D. Wilder, J.L. Burch, R.B. Torbert, P.-A. Lindqvist, D.B. Graham, R.J. Strangeway, O. Le Contel, J.C. Holmes, J.E. Stawarz, K.A. Goodrich, S. Eriksson, B.L. Giles, D. Gershman, L.J. Chen: Magnetic reconnection in three dimensions: Observations of electromagnetic drift waves in the adjacent current sheet, *J. Geophys. Res.*, **124**, 10104-10118, 2019.

Esposito, M., D.J. Armstrong, D. Gandolfi, V. Adibekyan, M. Fridlund, N.C. Santos, J.H. Livingston, E. Delgado Mena, L. Fossati, J. Lillo-Box, O. Barragán, D. Barrado, P.E. Cubillos, B. Cooke, A.B. Justesen, F. Meru, R.F. Díaz, F. Dai, L.D. Nielsen, C.M. Persson, P.J. Wheatley, A.P. Hatzes, V. Van Eylen, M.M. Musso, R. Alonso, P.G. Beck, S.C.C. Barros, D. Bayliss, A.S. Bonomo, F. Bouchy, D.J.A. Brown, E. Bryant, J. Cabrera, W.D. Cochran, S. Csizmadia, H. Deeg, O. Demangeon, M. Deleuil, X. Dumusque, P. Eigmüller, M. Endl, A. Erikson, F. Faedi, P. Figueira, A. Fukui, S. Grziwa, E.W. Guenther, D. Hidalgo, M. Hjorth, T. Hirano, S. Hojjatpanah, E. Knudstrup, J. Korth, K.W.F. Lam, J. de Leon, M.N. Lund, R. Luque, S. Mathur, P. Montañés Rodríguez, N. Narita, D. Nespral, P. Niraula, G. Nowak, H.P. Osborn, E. Pallé, M. Pätzold, D. Pollacco, J. Prieto-Arranz, H. Rauer, S. Redfield, I. Ribas, S.G. Sousa, A.M.S. Smith, M. Tala-Pinto, S. Udry, J.N. Winn: HD 219666 b: A hot-Neptune from TESS sector 1, *Astron. Astrophys.*, **623**, A165, 2019.

Fadanelli, S., B. Lavraud, F. Califano, C. Jacquey, Y. Vernisse, I. Kacem, E. Penou, D.J. Gershman, J. Dorelli, C. Pollock, B.L. Giles, L.A. Avanov, J. Burch, M.O. Chandler, V.N. Coffey, J.P. Eastwood, R. Ergun, C.J. Farrugia, S.A. Fuselier, V.N. Genot, E. Grigorenko, H. Hasegawa, Y. Khotyaintsev, O. Le Contel, A. Marchaudon, T.E. Moore, R. Nakamura, W.R. Paterson, T. Phan, A.C. Rager, C.T. Russell, Y. Saito, J.-A. Sauvaud, C. Schiff, S.E. Smith, S. Toledo Redondo, R.B. Torbert, S. Wang, S. Yokota: Four-spacecraft measurements of the shape and dimensionality of magnetic structures in the near-Earth plasma environment, *J. Geophys. Res.*, **124**, 6850-6868, 2019.

Fischer, G., J.A. Pagaran, P. Zarka, M. Delcroix, U.A. Dyudina, W.S. Kurth, D.A. Gurnett: Analysis of a long-lived, two-cell lightning storm on Saturn, *Astron. Astrophys.*, **621**, A113, 2019.

Fossati, L.: A glance into the end of a planetary system, *Science*, **364**, 25-26, 2019.

Freiherr von Forstner, J.L., J. Guo, R.F. Wimmer-Schweingruber, M. Temmer, M. Dumbovi, A. Veronig, C. Möstl, D.M. Hassler, C.J. Zeitlin, B. Ehresmann: Tracking and validating ICMEs propagating towards Mars using STEREO Heliospheric Imagers combined with Forbush decreases detected by MSL/RAD, *Space Weather*, **17**, 586-598, 2019.

Gachechiladze, T., T.V. Zaqarashvili, E. Gurgenashvili, G. Ramishvili, M. Carbonell, R. Oliver, J.L. Ballester: Magneto-Rossby waves in the solar tachocline and the annual variations in solar activity, *Astrophys. J.*, **874**, 162, 2019.

Gandolfi, D., L. Fossati, J.H. Livingston, K.G. Stassun, S Grziwa, O. Barragán, M. Fridlund, D. Kubyshkina, C.M. Persson, F. Dai, K.W.F. Lam, S. Albrecht, N. Batalha, P.G. Beck, A. Bo Justesen, J. Cabrera, S. Cartwright, W.D. Cochran, S. Csizmadia, M.D. Davies, H.J. Deeg, P. Eigmüller, M. Endl, A. Erikson, M. Esposito, R.A. García, R. Goeke, L. González-Cuesta, E.W. Guenther, A.P. Hatzes, D. Hidalgo, T. Hirano, M. Hjorth, P. Kabath, E. Knudstrup, J. Korth, J. Li, R. Luque, S. Mathur, P. Montañes Rodríguez, N. Narita, D. Nespral, P. Niraula, G. Nowak, E. Palle, M. Pätzold, J. Prieto-Arranz, H. Rauer, S. Redfield, I. Ribas, M. Skarka, A.M.S. Smith, P. Rowden, G. Torres, V. Van Eylen, M.L. Vezie: The transiting multi-planet system HD15337: Two nearly equal-mass planets straddling the radius gap, Astrophys. J. Lett., 876, L24, 2019.

Goetz, C., B.T. Tsurutani, P. Henri, M. Volwerk, E. Behar, N.J.T. Edberg, A. Eriksson, R. Goldstein, P. Mokashi, H. Nilsson, I. Richter, A. Wellbrock, K.-H. Glassmeier: Unusually high magnetic fields in the coma of 67P/Churyumov-Gerasimenko during its high-activity phase, Astron. Astrophys., 630, A38, 2019.

Good, S.W., E.K.J. Kilpua, A.T. LaMoury, R.J. Forsyth, J.P. Eastwood, C. Möstl: Self-similarity of ICME flux ropes: Observations by radially aligned spacecraft in the inner heliosphere, J. Geophys. Res., 124, 4960-4982, 2019.

Goodrich, K.A., R. Ergun, S.J. Schwartz, L.B. Wilson, A. Johlander, D. Newman, F.D. Wilder, J. Holmes, J. Burch, R. Torbert, Y. Khotyaintsev, P.-A. Lindqvist, R. Strangeway, D. Gershman, B. Giles: Impulsively reflected ions: A plausible mechanism for ion acoustic wave growth in collisionless shocks, J. Geophys. Res., 124, 1855-1865, 2019.

Güttler, C., T. Mannel, A. Rotundi, S. Merouane, M. Fulle, D. Bockelée-Morvan, J. Lasue, A.C. Levasseur-Regourd, J. Blum, G. Naletto, H. Sierks, M. Hilchenbach, C. Tubiana, F. Capaccioni, J.A. Paquette, A. Flandes, F. Moreno, J. Agarwal, D. Bodewits, I. Bertini, G.P. Tozzi, K. Hornung, Y. Langevin, H. Krüger, A. Longobardo, V. Della Corte, I. Tóth, G. Filacchione, S.L. Ivanovski, S. Mottola, G. Rinaldi: Synthesis of the morphological description of cometary dust at comet 67P/Churyumov-Gerasimenko, Astron. Astrophys., 630, A24, 2019.

Gvaramadze, V.V., Yu.V. Pakhomov, A.Y. Kniazev, T.A. Ryabchikova, N. Langer, L. Fossati, E.K. Grebel: TYC 8606-2025-1: A mild barium star surrounded by the ejecta of a very late thermal pulse, MNRAS, 489, 5136-5145, 2019.

Hasegawa, H., R.E. Denton, R. Nakamura, K.J. Genestreti, T.K.M. Nakamura, K.-J. Hwang, T.D. Phan, R.B. Torbert, J.L. Burch, B.L. Giles, D.J. Gershman, C.T. Russell, R.J. Strangeway, P.-A. Lindqvist, Y.V. Khotyaintsev, R.E. Ergun, N. Kitamura, Y. Saito: Reconstruction of the electron diffusion region of magnetotail reconnection seen by the MMS spacecraft on 11 July 2017, J. Geophys. Res., 124, 122-138, 2019.

Hellier, C., D.R. Anderson, A.H.M.J. Triaud, F. Bouchy, A. Burdanov, A. Collier Cameron, L. Delrez, D. Ehrenreich, M. Gillon, E. Jehin, M. Lendl, E. Linder, L.D. Nielsen, P.F.L. Maxted, F. Pepe, D. Pollacco, D. Queloz, D. Ségransan, B. Smalley, J.J. Spake, L.Y. Temple, S. Udry, R.G. West, A. Wyttenbach: WASP-166b: A bloated super-Neptune transiting a V=9 star, *MNRAS*, **488**, 3067-3075, 2019.

Hellier, C., D.R. Anderson, F. Bouchy, A. Burdanov, A. Collier Cameron, L. Delrez, M. Gillon, E. Jehin, M. Lendl, L.D. Nielsen, P.F.L. Maxted, F. Pepe, D. Pollacco, D. Queloz, D. Segransan, B. Smalley, A.H.M.J. Triaud, S. Udry, R.G. West: New transiting hot Jupiters discovered by WASP-South, Euler/CORALIE, and TRAPPIST-South, *MNRAS*, **482**, 1379-1391, 2019.

Hesse, M., C. Norgren, P. Tenfjord, J.L. Burch, Y.-H. Liu, L.-J. Chen, N. Bessho, S. Wang, R. Nakamura, J.P. Eastwood, M. Hoshino, R.B. Torbert, R.E. Ergun: Erratum: "On the role of separatrix instabilities in heating the reconnection outflow region" [Phys. Plasmas 25, 122902 (2018)], *Phys. Plasmas*, **26**, 049901, 2019.

Hinterreiter, J., J. Magdalenic, M. Temmer, C. Verbeke, I.C. Jebaraj, E. Samara, E. Asvestari, S. Poedts, J. Pomoell, E. Kilpua, L. Rodriguez, C. Scolini, A. Isavnin: Assessing the performance of EUHFORIA modeling the background solar wind, *Solar Phys.*, **294**, 170, 2019.

Hofer, B., Ph.-A. Bourdin: Application of the electromotive force as a shock front indicator in the inner heliosphere, *Astrophys. J.*, **878**, 30, 2019.

Holmes, J.C., R.E. Ergun, R. Nakamura, O. Roberts, F.D. Wilder, D.L. Newman: Structure of electron-scale plasma mixing along the dayside reconnection separatrix, *J. Geophys. Res.*, **124**, 8788–8803, 2019.

Hu, R.X., X. Shan, G.Y. Yuan, S.W. Wang, W.H. Zhang, W. Qi, Z. Cao, Y.R. Li, M.M. Chen, X.P. Yang, B. Wang, S.P. Shao, F. Li, X.Q. Zhong, D. Fan, X.J. Hao, C.Q. Feng, Z.P. Su, C.L. Shen, X. Li, G.Y. Dai, B.L. Qiu, Z.H. Pan, K. Liu, C.K. Xu, S.B. Liu, Q. An, T.L. Zhang, Y.M. Wang: A low-energy ion spectrometer with half-space entrance for three-axis stabilized spacecraft, *Sci. China Technol. Sci.*, **62**, 1015–1027, 2019.

Imai, M., A. Lecacheux, T.E. Clarke, C.A. Higgins, M. Panchenko, V.V. Zakharenko, A.I. Brazhenko, A.V. Frantsuzenko, O.N. Ivantyshin, A.A. Konovalenko, V.V. Koshovyy: Concurrent Jovian S-burst beaming as observed from LWA1, NDA, and Ukrainian radio telescopes, *J. Geophys. Res.*, **124**, 5302-5316, 2019.

Janvier, M., R.M. Winslow, S. Good, E. Bonhomme, P. Démoulin, S. Dasso, C. Möstl, N. Lugaz, T. Amerstorfer, E. Soubrié, P.D. Boakes: Generic magnetic field intensity profiles of interplanetary Coronal Mass Ejections at Mercury, Venus, and Earth from superposed epoch analyses, *J. Geophys. Res.*, **124**, 812-836, 2019.

Johnstone, C.P., M.L. Khodachenko, T. Lüftinger, K.G. Kislyakova, H. Lammer, M. Güdel: Extreme hydrodynamic losses of Earth-like atmospheres in the habitable zones of very active stars, *Astron. Astrophys.*, **624**, L10, 2019.

Kallio, E., S. Dyadechkin, P. Wurz, M.L. Khodachenko: Space weathering on the Moon: Farside-nearside solar wind precipitation asymmetry, *Planet. Space Sci.*, **166**, 9-22, 2019.

Khodachenko, M.L., I.F. Shaikhislamov, H. Lammer, A.G. Berezutsky, I.B. Miroshnichenko, M.S. Rumenskikh, K.G. Kislyakova, N.K. Dwivedi: Global 3D hydrodynamic modeling of in-transit Lyα absorption of GJ 436b, *Astrophys. J.*, **885**, 67, 2019.

Kislyakova, K.G., M. Holmström, P. Odert, H. Lammer, N.V. Erkaev, M.L. Khodachenko, I.F. Shaikhislamov, E. Dorfi, M. Güdel: Transit Lyman-α signatures of terrestrial planets zones of M dwarfs, *Astron. Astrophys.*, **623**, A131, 2019.

Kömle, N.I., P. Tiefenbacher, C. Pitcher, L. Richter, T. Tattusch, R. Paul: Sampling of Mars analogue materials in a laboratory environment, *Acta Geotechnica*, **14**, 429-442, 2019.

Korovinskiy, D.B., A.V. Divin, V.S. Semenov, N.V. Erkaev, I.B. Ivanov, S.A. Kiehas, S. Markidis: The transition from "double-gradient" to ballooning unstable mode in bent magnetotail-like current sheet, *Phys. Plasmas*, **26**, 102901, 2019.

Kubyshkina, D., L. Fossati, A.J. Mustill, P.E. Cubillos, M.B. Davies, N.V. Erkaev, C.P. Johnstone, K.G. Kislyakova, H. Lammer, M. Lendl, P. Odert: The Kepler-11 system: Evolution of the stellar high-energy emission and initial planetary atmospheric mass fractions, *Astron. Astrophys.*, **632**, A65, 2019.

Kubyshkina, D., P.E. Cubillos, L. Fossati, N.V. Erkaev, C.P. Johnstone, K.G. Kislyakova, H. Lammer, M. Lendl, P. Odert, M. Güdel: Close-in sub-Neptunes reveal the past rotation history of their host stars: Atmospheric evolution of planets in the HD 3167 and K2-32 planetary systems, *Astrophys. J.*, **879**, 26, 2019.

Kucharski, D., G. Kirchner, T Otsubo, H. Kunimori, M.K. Jah, F. Koidl, J.C. Bennett, H.-C. Lim, P. Wang, M. Steindorfer, K. Sosnica: Hypertemporal photometric measurement of spaceborne mirrors specular reflectivity for Laser Time Transfer link model, *Adv. Space Res.*, **64**, 957-963, 2019.

Kuridze, D., M. Mathioudakis, H. Morgan, R. Oliver, L. Kleint, T.V. Zaqarashvili, A. Reid, J. Koza, M.G. Löfdahl, T. Hillberg, V. Kukhianidze, A. Hanslmeier: Mapping the magnetic field of flare coronal loops, *Astrophys. J.*, **874**, 126, 2019.

Lammer, H., L. Sproß, J.L. Grenfell, M. Scherf, L. Fossati, M. Lendl, P.E. Cubillos: The role of N2 as a geo-biosignature for the detection and characterization of Earth-like habitats, *Astrobiol.*, **19**, 927-950, 2019.

Lanza, A.F., L. Gizon, T.V. Zaqarashvili, Z.-C. Liang, K. Rodenbeck: Sectoral r modes and periodic radial velocity variations of Sun-like stars, *Astron. Astrophys.*, **623**, A50, 2019.

Lasue, J., I. Maroger, R. Botet, Ph. Garnier, S. Merouane, T. Mannel, A.C. Levasseur-Regourd, M.S. Bentley: Flattened loose particles from numerical simulations compared to particles collected by Rosetta, *Astron. Astrophys.*, **630**, A28, 2019.

Lendl, M.: High precision ground-based photometry with 1-m class telescopes, *Contrib. Astron. Obs. Skalnaté Pleso*, **49**, 107-118, 2019.

Lendl, M., D.R. Anderson, A. Bonfanti, F. Bouchy, A. Burdanov, A. Collier Cameron, L. Delrez, M. Gillon, C. Hellier, E. Jehin, P.F.L. Maxted, L. Dyregaard Nielsen, F. Pepe, D. Pollacco, D. Queloz, D. Ségransan, J. Southworth, B. Smalley, S. Thompson, O. Turner, A.H.M.J. Triaud, S. Udry, R.G. West: WASP-147b, 160Bb, 164b, and 165b: Two hot Saturns and two Jupiters, including two planets with metal-rich hosts, *MNRAS*, **482**, 301-312, 2019.

Lhotka, C., C. Gales: Charged dust close to outer mean-motion resonances in the heliosphere, *Cel. Mech. Dyn. Astron.*, **131**, 49, 2019.

Lhotka, C., Ph.-A. Bourdin, E. Pilat-Lohinger: Orbital stability of ensembles of particles in regions of magnetic reconnection in Earth's magneto-tail, *Phys. Plasmas*, **26**, 072903, 2019.

Lhotka, C., Y. Narita: Kinematic models of the interplanetary magnetic field, *Ann. Geophys.*, **37**, 299-314, 2019.

Macher, W., N. Kömle, Y. Skorov, L. Rezac, G. Kargl, P. Tiefenbacher: 3D thermal modeling of two selected regions on comet 67P and comparison with Rosetta/MIRO measurements, *Astron. Astrophys.*, **630**, A12, 2019.

Mallonn, M., C. von Essen, E. Herrero, X. Alexoudi, T. Granzer, M. Sosa, K.G. Strassmeier, G. Bakos, D. Bayliss, R. Brahm, M. Bretton, F. Campos, L. Carone, K.D. Colón, H.A. Dale, D. Dragomir, N. Espinoza, P. Evans, F. Garcia, S.-H. Gu, P. Guerra, Y. Jongen, A. Jordán, W. Kang, E. Keles, T. Kim, M. Lendl, D. Molina, M. Salisbury, F. Scaggiante, A. Shporer, R. Siverd, E. Sokov, I. Sokova, A. Wünsche: Ephemeris refinement of 21 hot Jupiter exoplanets with high timing uncertainties, *Astron. Astrophys.*, **622**, A81, 2019.

Mancini, L., J. Southworth, P. Molliere, J. Tregloan-Reed, I.G. Juvan, G. Chen, P. Sarkis, I. Bruni, S. Ciceri, M.I. Andersen, V. Bozza, D.M. Bramich, M. Burgdorf, G. D'Ago, M. Dominik, D.F. Evans, R. Figuera Jaimes, L. Fossati, Th. Henning, T.C. Hinse, M. Hundertmark, U.G. Jørgensen, E. Kerins, H. Korhonen, M. Küffmeier, P. Longa, N. Peixinho, A. Popovas, M. Rabus, S. Rahvar, J. Skottfelt, C. Snodgrass, R. Tronsgaard, Y. Wang, O. Wertz: Physical properties and transmission spectrum of the WASP-74 planetary system from multiband photometry, *MNRAS*, **485**, 5168-5179, 2019.

Mannel, T., M.S. Bentley, P.D. Boakes, H. Jeszenszky, P. Ehrenfreund, C. Engrand, C. Koeberl, A.C. Levasseur-Regourd, J. Romstedt, R. Schmied, K. Torkar, I. Weber: Dust of comet 67P/Churyumov-Gerasimenko collected by Rosetta/MIDAS: Classification and extension to the nanometer scale, *Astron. Astrophys.*, **630**, A26, 2019.

Masunaga, K., Y. Futaana, M. Persson, S. Barabash, T.L. Zhang, Z.J. Rong, A.Fedorov: Effects of the solar wind and the solar EUV flux on O+ escape rates from Venus, *Icarus*, **321**, 379-387, 2019.

Mathew, M., B.G. Nair, M. Safonova, S. Sriram, A. Prakash, M. Sarpotdar, S. Ambily, K. Nirmal, A.G. Sreejith, J. Murthy, P.U. Kamath, S. Kathiravan, B.R. Prasad, N. Brosch, N. Kappelmann, N. Suraj Gadde, R. Narayan: Prospect for UV observations from the Moon. III. Assembly and ground calibration of Lunar Ultraviolet Cosmic Imager (LUCI), *Astrophys. Space Sci.*, **364**, 53, 2019.

Merkin, V.G., E.V. Panov, K.A. Sorathia, A.Y. Ukhorskiy: Contribution of bursty bulk flows to the global dipolarization of the magnetotail during an isolated substorm, *J. Geophys. Res.*, **124**, 8647–8668, 2019.

Nakamura, R., K.J. Genestreti, T.K.M. Nakamura, W. Baumjohann, A. Varsani, T. Nagai, N. Bessho, J.L. Burch, R.E. Denton, J.P. Eastwood, R.E. Ergun, D.J. Gershman, B.L. Giles, H. Hasegawa, M. Hesse, P.-A. Lindqvist, C.T. Russell, J.E. Stawarz, R.J. Strangeway, R.B. Torbert: Structure of the current sheet in the 11 July 2017 electron diffusion region event, *J. Geophys. Res.*, **124**, 1173-1186, 2019.

Nakamura, T.K.M., T. Umeda, R. Nakamura, H.S. Fu, M. Oka: Disturbance of the front region of magnetic reconnection outflow jets due to the lower-hybrid drift instability, *Phys. Rev. Lett.*, **123**, 235101, 2019.

Nakamura, Y., Y. Kasaba, T. Kimura, L. Lamy, B. Cecconi, G. Fischer, A. Sasaki, C. Tao, F. Tsuchiya, H. Misawa, A. Kumamoto, A. Morioka: Seasonal variation of north-south asymmetry in the intensity of Saturn Kilometric Radiation from 2004 to 2017, *Planet. Space Sci.*, **178**, 104711, 2019.

Narita, Y.: A note on Capon's minimum variance projection for multi-spacecraft data analysis, *Front. Physics*, **7**, 8, 2019.

Narita, Y., W. Baumjohann, R.A. Treumann: Scaling laws in Hall inertial-range turbulence, *Ann. Geophys.*, **37**, 825-834, 2019.

Nielsen, L.D., F. Bouchy, O.D. Turner, D.R. Anderson, K. Barkaoui, Z. Benkhaldoun, A. Burdanov, A. Collier Cameron, L. Delrez, M. Gillon, E. Ducrot, C. Hellier, E. Jehin, M. Lendl, P.F.L. Maxted, F. Pepe, D. Pollacco, F.J. Pozuelos, D. Queloz, D. Ségransan, B. Smalley, A.H.M.J. Triaud, S. Udry, R.G. West: WASP-169, WASP-171, WASP-175, and WASP-182: Three hot Jupiters and one bloated sub-Saturn mass planet discovered by WASP-South, *MNRAS*, **489**, 2478-2487, 2019.

O`Rourke, L., C. Tubiana, C. Güttler, S. Lodiot, P. Muñoz, A. Herique, Y. Rogez, J. Durand, A. Charpentier, H. Sierks, P. Gutierrez-Marques, J. Deller, B. Grieger, R. Andres, B. Geiger, K. Geurts, S. Ulamec, N. Kömle, V. Lommatsch, M. Maibaum, J.L. Pellon, C. Bielsa, R. Garmier, M. Taylor, P. Martin, M. Küppers, A. Accomazzo, V. Companys, J.P. Bibring, W. Kofman, S. Mckenna Lawlor, M. Salatti, P. Gaudon: The search campaign to identify and image the Philae Lander on the surface of comet 67P/Churyumov-Gerasimenko, *Acta Astronaut.*, **157**, 199-214, 2019.

Pan, Z.H., G.Q. Wang, L.F. Meng, Z. Yi, T.L. Zhang: Influence of Alfvénic characteristics on calibration of satellite magnetometer, *Chin. J. Geophys.*, **62**, 1193-1198, 2019.

Panov, E.V., W. Baumjohann, R. Nakamura, J.M. Weygand, B.L. Giles, C.T. Russel, G. Reeves, M.V. Kubyshkina: Continent-wide R1/R2 current system and Ohmic losses by broad dipolarization-injection fronts, *J. Geophys. Res.*, **124**, 4064-4082, 2019.

Panov, E.V., W. Baumjohann, R. Nakamura, P.L. Pritchett, J.M. Weygand, M.V. Kubyshkina: Ionospheric footprints of detached magnetotail interchange heads, *Geophys. Res. Lett.*, **46**, 7237-7247, 2019.

Pass, E.K., N.B. Cowan, P.E. Cubillos, J.G. Sklar: Estimating dayside effective temperatures of hot Jupiters and associated uncertainties through Gaussian process regression, *MNRAS*, **489**, 941-950, 2019.

Pearlman, M.R., C.E. Noll, E.C. Pavlis, F.G. Lemoine, L. Combrink, J.J. Degnan, G. Kirchner, U. Schreiber: The ILRS: Approaching 20 years and planning for the future, *J. Geodesy*, **93**, 2161-2180, 2019.

Pérez-de-Tejada, H., R. Lundin, Y. Futaana, T.L. Zhang: Measurement of plasma channels in the Venus wake, *Icarus*, **321**, 1026-1037, 2019.

Persson, M., Y. Futaana, H. Nilsson, G. Stenberg Wieser, M. Hamrin, A. Fedorov, T.L. Zhang, S. Barabash: Heavy ion flows in the upper ionosphere of the Venusian north pole, *J. Geophys. Res.*, **124**, 4597-4607, 2019.

Petit, V., G.A. Wade, F.R.N Schneider, L. Fossati, K. Kamp, C. Neiner, A. David-Uraz, E. Alecian, MiMeS Collaboration: The MiMeS survey of magnetism in massive stars: Magnetic properties of the O-type star population, *MNRAS*, **489**, 5669–5687, 2019.

Plaschke, F.: How many solar wind data are sufficient for accurate fluxgate magnetometer offset determinations?, *Geosci. Instrum. Method. Data Syst.*, **8**, 285-291, 2019.

Plaschke, F., H.-U. Auster, D. Fischer, K.-H. Fornaçon, W. Magnes, I. Richter, D. Constantinescu, Y. Narita: Advanced calibration of magnetometers on spin-stabilized spacecraft based on parameter decoupling, *Geosci. Instrum. Method. Data Syst.*, **8**, 63-76, 2019.

Poh, G., J.A. Slavin, S. Lu, G. Le, D.S. Ozturk, W.-J. Sun, S. Zou, J.P. Eastwood, R. Nakamura, W. Baumjohann, C.T. Russell, D.J. Gershman, B.L. Giles, C.J. Pollock, T.E. Moore, R.B. Torbert, J.L. Burch: Dissipation of earthward propagating flux rope through re-reconnection with geomagnetic field: An MMS case study, *J. Geophys. Res.*, **124**, 7477-7493, 2019.

Reiss, M.A., P.J. MacNeice, L.M. Mays, C.N. Arge, C. Möstl, L. Nikolic, T. Amerstorfer: Forecasting the ambient solar wind with numerical models. I. On the implementation of an operational framework, *Astrophys. J. Suppl. Ser.*, **240**, 35, 2019.

Roberts, O.W., Y. Narita, R. Nakamura, Z. Vörös, D. Gershman: Anisotropy of the spectral index in ion scale compressible turbulence: MMS observations in the magnetosheath, *Front. Physics*, **7**, 184, 2019.

Rozhnoi, A., M. Solovieva, V. Fedun, P. Gallagher, J. McCauley, M.Y. Boudjada, S. Shelyag, H.U. Eichelberger: Strong influence of solar X-ray flares on low-frequency electromagnetic signals in middle latitudes, *Ann. Geophys.*, **37**, 843-850, 2019.

Salz, M., P.C. Schneider, L. Fossati, S. Czesla, K. France, J.H.M.M. Schmitt: Swift UVOT near-UV transit observations of WASP-121 b, *Astron. Astrophys.*, **623**, A57, 2019.

Schmid, D., M. Volwerk, F. Plaschke, R. Nakamura, W. Baumjohann, G.Q. Wang, M.Y. Wu, T.L. Zhang: A statistical study on the properties of dips ahead of dipolarization fronts observed by MMS, *J. Geophys. Res.*, **124**, 139-150, 2019.

Schmid, D., M. Volwerk, F. Plaschke, R. Nakamura, W. Baumjohann, G.Q. Wang, M.Y. Wu, T.L. Zhang: Dipolarization fronts: Tangential discontinuities? On the spatial range of validity of the MHD jump conditions, *J. Geophys. Res.*, **124**, 9963–9975, 2019.

Seidel, J.V., D. Ehrenreich, A. Wyttenbach, R. Allart, M. Lendl, L. Pino, V. Bourrier, H. M. Cegla, C. Lovis, D. Barrado, D. Bayliss, N. Astudillo-Defru, A. Deline, C. Fisher, K. Heng, R. Joseph, B. Lavie, C. Melo, F. Pepe, D. Ségransan, S. Udry: Hot exoplanet atmospheres resolved with transit spectroscopy (HEARTS)? II. A broadened sodium feature on the ultra-hot giant WASP-76b, *Astron. Astrophys.*, **623**, A166, 2019.

Sergeev, V.A., S.V. Apatenkov, R. Nakamura, W. Baumjohann, Y.V. Khotyaintsev, K. Kauristie , M. van de Kamp, J.L. Burch, R.E. Ergun, P.-A. Lindqvist, R. Torbert, C.T. Russell, B.L. Giles: Substorm-related near-Earth reconnection surge: Combining telescopic and microscopic views, *Geophys. Res. Lett.*, **46**, 6239-6247, 2019.

Shi, J., Z. Zhang, K. Torkar, Z. Cheng, P. Escoubet, A. Farzakeley, M. Dunlop, C. Carr: South-north hemispheric asymmetry of the FAE distribution around the cusp region: Cluster observation, *J. Geophys. Res.*, **124**, 5342-5352, 2019.

Sitnov, M., J. Birn, B. Ferdousi, E. Gordeev, Y. Khotyaintsev, V. Merkin, T. Motoba, A. Otto, E.V. Panov, P. Pritchett, F. Pucci, J. Raeder, A. Runov, V. Sergeev, M. Velli, X. Zhou: Explosive magnetotail activity, *Space Sci. Rev.*, **215**, 31, 2019.

Sorriso-Valvo, L., F. Catapano, A. Retinò, O. Le Contel, D. Perrone, O.W. Roberts, J.T. Coburn, V. Panebianco, F. Valentini, S. Perri, A. Greco, F. Malara, V. Carbone, P. Veltri, O. Pezzi, F. Fraternale, F. Di Mare, R. Marino, B. Giles, T.E. Moore, C.T. Russell, R.B. Torbert, J.L. Burch, Yu.V. Khotyaintsev: Turbulence-driven ion beams in the magnetospheric Kelvin-Helmholtz instability, *Phys. Rev. Lett.*, **122**, 035102, 2019.

Sreejith, A.G., L. Fossati, B.T. Fleming, K.C. France, T.T. Koskinen, A. Egan, H.T. Rüdisser, M. Steller: Colorado Ultraviolet Transit Experiment data simulator, *J. Astron. Telesc. Instrum. Syst.*, **5**, 018004, 2019.

Stawarz, J.E., J.P. Eastwood, T.D. Phan, I.L. Gingell, M.A. Shay, J.L. Burch, R.E. Ergun, B.L. Giles, D.J. Gershman, O. Le Contel, P.-A. Lindqvist, C.T. Russell, R.J. Strangeway, R.B. Torbert, M.R. Argall, D. Fischer, W. Magnes, L. Franci: Properties of the turbulence associated with electron-only magnetic reconnection in Earth's magnetosheath, *Astrophys. J. Lett.*, **877**, L37, 2019.

Steindorfer, M.A., G. Kirchner, F. Koidl, P. Wang, H. Wirnsberger, E. Schoenemann, F. Gonzalez: Attitude determination of Galileo satellites using high-resolution kHz SLR, *J. Geodesy*, **93**, 1845-1851, 2019.

Sulis, S., D. Dragomir, M. Lendl, V. Bourrier, B.O. Demory, L. Fossati, P.E. Cubillos, D.B. Guenther, S.R. Kane, R. Kuschnig, J.M. Matthews, A.F.J. Moffat, J.F. Rowe, D. Sasselov, W.W. Weiss, J.N. Winn: Multi-season optical modulation phased with the orbit of the super-Earth 55 Cancri e, *Astron. Astrophys.*, **631**, A129, 2019.

Sun, W.J., J.A. Slavin, A.M. Tian, S.C. Bai, G.K. Poh, M. Akhavan-Tafti, San Lu, S.T. Yao, G. Le, R. Nakamura, B.L. Giles, J.L. Burch: MMS study of the structure of ion-scale flux ropes in the Earth's cross-tail current sheet, *Geophys. Res. Lett.*, **46**, 6168-6177, 2019.

Temple, L.Y., C. Hellier, Y. Almleaky, D.R. Anderson, F. Bouchy, D.J.A. Brown, A. Burdanov, A. Collier Cameron, L. Delrez, M. Gillon, E. Jehin, M. Lendl, P.F.L. Maxted, C. Murray, L.D. Nielsen, F. Pepe, D. Pollacco, D. Queloz, D. Ségransan, B. Smalley, S. Thompson, A.H.M.J. Triaud, O.D. Turner, S. Udry, R.G. West: WASP-190b: Tomographic discovery of a transiting Hot Jupiter, *Astron. J.*, **157**, 141, 2019.

Toledo-Redondo, S., B. Lavraud, S.A. Fuselier, M. André, Yu.V. Khotyaintsev, R. Nakamura, C.P. Escoubet, W.Y. Li, K. Torkar, F. Cipriani, A.C. Barrie, B. Giles, T.E. Moore, D. Gershman, P.-A. Lindqvist, R.E. Ergun, C. T. Russell, J.L. Burch: Electrostatic spacecraft potential structure and wake formation effects for characterization of cold ion beams in the Earth's magnetosphere, *J. Geophys. Res.*, **124**, 10048–10062, 2019.

Torkar, K., R. Nakamura, S. Wellenzohn, H. Jeszenszky, R.B. Torbert, P.-A. Lindqvist, R.E. Ergun, B.L. Giles: Improved determination of plasma density based on spacecraft potential of the Magnetospheric Multiscale mission under active potential control, *IEEE Trans. Plasma Sci.*, **47**, 3636-3647, 2019.

Treumann, R.A., W. Baumjohann: Possible increased critical temperature Tc in anisotropic bosonic gases, *Sci. Rep.*, **9**, 10339, 2019.

Treumann, R.A., W. Baumjohann: A note on the entropy force in kinetic theory and black holes, *Entropy*, **21**, 716, 2019.

Treumann, R.A., W. Baumjohann: Electron pairing in mirror modes: Surpassing the quasi-linear limit, *Ann. Geophys.*, **37**, 971-988, 2019.

Treumann, R.A., W. Baumjohann, Y. Narita: On the ion-inertial-range density-power spectra in solar wind turbulence, *Ann. Geophys.*, **37**, 183-199, 2019.

Treumann, R.A., W. Baumjohann, Y. Narita: On the applicability of Taylor's hypothesis in streaming magnetohydrodynamic turbulence, *Earth Planets Space*, **71**, 41, 2019.

Turc, L., O.W. Roberts, M.O. Archer, M. Palmroth, M. Battarbee, T. Brito, U. Ganse, M. Grandin, Y. Pfau-Kempf, C.P. Escoubet, I. Dandouras: First observations of the disruption of the Earth's foreshock wave field during magnetic clouds, *Geophys. Res. Lett.*, **46**, 12644-12653, 2019.

Turner, O.D., D.R. Anderson, K. Barkaoui, F. Bouchy, Z. Benkhaldoun, D.J.A. Brown, A. Burdanov, A. Collier Cameron, E. Ducrot, M. Gillon, C. Hellier, E. Jehin, M. Lendl, P.F.L. Maxted, L.D. Nielsen, F. Pepe, D. Pollacco, F.J. Pozuelos, D. Queloz, D. Segransan, B. Smalley, A.H.M.J. Triaud, S. Udry, R.G. West: Three hot-Jupiters on the upper edge of the mass-radius distribution: WASP-177, WASP-181, and WASP-183, *MNRAS*, **485**, 5790-5799, 2019.

Vashalomidze, Z.M., T.V. Zaqarashvili, V.D. Kukhianidze: Measurement of the polytropic index during solar coronal rain using a diagram of the electron density distribution as a function of electron temperature, *Astrophys.*, **62**, 69-78, 2019.

Vashalomidze, Z.M., T.V. Zaqarashvili, V.D. Kukhianidze, G.T. Ramishvili: Eruption of prominences triggered by coronal rain in the solar atmosphere observed by SDO/AIA and Stereo/EUVI, *Astrophys.*, **62**, 529-539, 2019.

Vida, K., M. Leitzinger, L. Kriskovics, B. Seli, P. Odert, O.E. Kovács, H. Korhonen, L. van Driel-Gesztelyi: The quest for stellar coronal mass ejections in late-type stars I. Investigating Balmer-line asymmetries of single stars in Virtual Observatory data, *Astron. Astrophys.*, **623**, A49, 2019.

Volwerk, M., C. Goetz, E. Behar, M. Delva, N.J.T. Edberg, A. Eriksson, P. Henri, K. Llera, H. Nilsson, I. Richter, G. Stenberg Wieser, K.-H. Glassmeier: Dynamic field line draping at comet 67P/Churyumov-Gerasimenko during the Rosetta dayside excursion, *Astron. Astrophys.*, **630**, A44, 2019.

von Boetticher, A., A.H.M.J. Triaud, D. Queloz, S. Gill, P.F.L. Maxted, Y. Amleaky, D.R. Anderson, F. Bouchy, A. Burdanov, A.C. Cameron, L. Delrez, E. Ducrot, F. Faedi, M. Gillon, Y.G.M. Chew, L. Hebb, C. Hellier, E. Jehin, M. Lendl, M. Marmier, D.V. Martin, J. McCormac, F. Pepe, D. Pollacco, D. Segransan, B. Smalley, S. Thompson, O. Turner, S. Udry, V. Van Grootel, R. West: The EBLM project. V. Physical properties of ten fully convective, very-low-mass stars, *Astron. Astrophys.*, **625**, A150, 2019.

Vorburger, A., M. Pfleger, J. Lindkvist, M. Holmström, H. Lammer, H.I.M. Lichtenegger, A. Galli, M. Rubin, P. Wurz: Three-dimensional modeling of Callisto's surface sputtered exosphere environment, *J. Geophys. Res.*, **124**, 7157-7169, 2019.

Vörös, Z., E. Yordanova, D.B. Graham, Y.V. Khotyaintsev, Y. Narita: MMS observations of whistler and lower hybrid drift waves associated with magnetic reconnection in the turbulent magnetosheath, *J. Geophys. Res.*, **124**, 8551–8563, 2019.

Vörös, Z., E. Yordanova, Y.V. Khotyaintsev, A. Varsani, Y. Narita: Energy conversion at kinetic scales in the turbulent magnetosheath, *Front. Astron. Space Sci.*, **6**, 60, 2019.

Vršnak, B., T. Amerstorfer, M. Dumbović, M. Leitner, A.M. Veronig, M. Temmer, C. Möstl, U.V. Amerstorfer, C.J. Farrugia, A.B. Galvin: Heliospheric evolution of magnetic clouds, *Astrophys. J.*, **877**, 77, 2019.

Vuorinen, L., H. Hietala, F. Plaschke: Jets in the magnetosheath: IMF control of where they occur, *Ann. Geophys.*, **37**, 689-697, 2019.

Wang, G., T.L. Zhang, Z.L. Gao, M.Y. Wu, G.Q. Wang, D. Schmid: Propagation of EMIC waves inside the plasmasphere: A two-event study, *J. Geophys. Res.*, **124**, 8396–8415, 2019.

Wang, G.Q., T.L. Zhang, M.Y. Wu, D. Schmid, J.B. Cao, M. Volwerk: Solar wind directional change triggering flapping motions of the current sheet: MMS observations, *Geophys. Res. Lett.*, **46**, 64-70, 2019.

Wedlund, C.S., E. Behar, H. Nilsson, M. Alho, E. Kallio, H. Gunell, D. Bodewits, K. Heritier, M. Galand, A. Beth, M. Rubin, K. Altwegg, M. Volwerk, G. Gronoff, R. Hoekstra: Solar wind charge exchange in cometary atmospheres. III. Results from the Rosetta mission to comet 67P/Churyumov-Gerasimenko, *Astron. Astrophys.*, **630**, A37, 2019.

Weiss, A.J., A. Schneider, R. Sgier, T. Kacprzak, A. Amaraa, A. Refregier: Effects of baryons on weak lensing peak statistics, *JCAP*, **10**, 011, 2019.

Wilkinson, M. U. Schreiber, I. Procházka, C. Moore, J. Degnan, G. Kirchner, Z.P. Zhang, P. Dunn, V. Shargorodskiy, M. Sadovnikov, C. Courde, H. Kunimori: The next generation of satellite laser ranging systems, *J. Geodesy*, **93**, 2227-2247, 2019.

Wirnsberger, H., S. Krauss, T. Mayer-Gürr: First independent Graz Lunar Gravity Model derived from GRAIL, *Icarus*, **317**, 324-336, 2019.

Xu, Q., X. Xu, Q. Chang, Z. Rong, J. Wang, J. Xu, T.L. Zhang: Observations of the Venus dramatic response to an extremely strong interplanetary Coronal Mass Ejection, *Astrophys. J.*, **876**, 84, 2019.

Zhang, L.Q., W. Baumjohann, L. Dai, Yu.V. Khotyaintsev, C. Wang: Measurements of the vorticity in the bursty bulk flows, *Geophys. Res. Lett.*, **46**, 10322-10329, 2019.

Zhou, B., B. Cheng, X. Gou, L. Li, Y. Zhang, J. Wang, W. Magnes, R. Lammegger, A. Pollinger, M. Ellmeier, Q. Xiao, X. Zhu, S. Yuan, Y. Yang, X. Shen: First in-orbit results of the vector magnetic field measurement of the High Precision Magnetometer onboard the China Seismo-Electromagnetic Satellite, *Earth Planets Space*, **71**, 119, 2019.

BOOKS

Morbidelli, A., M. Blanc, Y. Alibert, L. Elkins-Tanton, P. Estrada, K. Hamano, H. Lammer, S. Raymond, M. Schönbächler (Eds.): The Delivery of Water to Protoplanets, Planets and Satellites, Springer, New York, 450 pages, 2019.

PROCEEDINGS & BOOK CHAPTERS

Aplin, K., G. Fischer: Atmospheric electricity in the solar system. In: *Oxford Research Encyclopedia of Planetary Science*, Ed. Read, P., Oxford University Press, Oxford, 29 p., 2019.

Benevenuti, F., E. Chielle, J. Tonfat, L. Tambara, F. Lima Kastensmidt, C.A. Zaffari, J.B. dos Santos Martins, O.S. Cupertino Durão: Experimental applications on SRAM-based FPGA for the NanosatC-BR2 scientific mission. In: *Proceedings 2019 IEEE International Parallel and Distributed Processing Symposium Workshops (IPDPSW)*, IEEE, Washington, 140-146, 2019.

Brown, P., U. Auster, J.E.S. Bergman, J. Fredriksson, Y. Kasaba, M. Mansour, A. Pollinger, R. Baughen, M. Berglund, D. Hercik, H. Misawa, A. Retino, M. Bendyk, W. Magnes, B. Cecconi, M.K. Dougherty, G. Fischer: Meeting the magnetic EMC challenges for the in-situ field measurements on the Juice mission. In: *Proceedings of the 2019 ESA Workshop on Aerospace EMC*, IEEE, New York, 6 p., 2019.

Jilete, B., T. Flohrer, T. Schildknecht, C. Paccolat, M. Steindorfer: Expert Centres: A key component in ESA's topology for space surveillance. In: *Proceedings, 1st NEO and Debris Detection Conference*, Eds. Flohrer, T., R. Jehn, F. Schmitz, ESA Space Safety Programme Office, Darmstadt, 6 p., 2019.

Kloth, A., J. Steinborn, T. Schildknecht, M. Steindorfer, F. Koidl, G. Kirchner: On the Horizon: New ESA Laser Ranging Station (ELRS) with debris tracking capabilities. In: *Proceedings, 1st NEO and Debris Detection Conference*, Eds. Flohrer, T., R. Jehn, F. Schmitz, ESA Space Safety Programme Office, Darmstadt, 3 p., 2019.

Nesterov, S., V. Denisenko, M.Y. Boudjada, H. Lammer: The influence of the magnetic field inclination on the quasistationary electric field penetration from the ground to the ionosphere. In: T*rigger Effects in Geosystems, Springer Proceedings in Earth and Environmental Sciences*, Eds. Kocharyan, G., A. Lyakhov, Springer Nature, Switzerland, 559-567, 2019.

Sánchez-Lavega, A., G. Fischer, L.N. Fletcher, E. García-Melendo, B. Hesman, S. Pérez-Hoyos, K.M. Sayanagi, L.A. Sromovsky: The Great Saturn Storm of 2010-2011. In: *Saturn in the 21st Century*, Eds. Baines, K.H., F.M. Flasar, N. Krupp, T. Stallard, Cambridge University Press, Cambridge, UK, 377-416, 2019.

Scherzer, M., M. Auer, A. Valavanoglou, S. Leitner, W. Magnes: Circuit design and verification method of integrated sensor-front-end elements for spaceborne fluxgate magnetometers. In: *Proc. 2019 15th Conference in PhD Research in Microelectronics and Electronics (PRIME)*, IEEE, New York, 181-184, 2019.

Steindorfer, M., G. Kirchner, F. Koidl, P. Wang: Recent space debris related activities at the SLR station Graz. In: *Proceedings, 1st NEO and Debris Detection Conference*, Eds. Flohrer, T., R. Jehn, F. Schmitz, ESA Space Safety Programme Office, Darmstadt, 5 p., 2019.

Sulis, S., D. Mary, L. Bigot: 3D magneto-hydrodynamic simulations to counteract the convective noise source for extrasolar planet detection. In: *Proceedings of the Annual meeting of the French Society of Astronomy and Astrophysics (SF2A-2019)*, Eds. Di Matteo, P., O. Creevey, A. Crida, G. Kordopatis, J. Malzac, J.-B. Marquette, M. N'Diaye, O. Venot, Société Francaise d'Astronomie et d'Astrophysique, Paris, 457-461, 2019.

For oral presentations and posters please refer to the "Publications" menu on www.iwf.oeaw.ac.at.

PERSONNEL

Agú, Martin A., Dipl.-Ing.
Aickara Gopinathan, Sreejith, Dr.
Amerstorfer, Tanja, Dr.
Arkhypov, Oleksiy, Dr.
Aydogar, Özer, Dipl.-Ing.
Bauer, Maike, BSc
Baumjohann, Wolfgang, Prof.
Bailey, Rachel L., Dr.
Berghofer, Gerhard, Ing.
Besser, Bruno P., Dr.
Boudjada, Mohammed Y., Dr.
Cubillos, Patricio E., Dr.
Delva, Magda, Dr.
Dwivedi, Navin K., Dr.
Eichelberger, Hans U., Dr.
Ellmeier, Michaela, Dr.
Fischer, David, Dipl.-Ing.
Fischer, Georg, Dr.
Flock, Barbara, Mag.
Fossati, Luca, Doz.
Fremuth, Gerhard, Dipl.-Ing.
Giner, Franz, Dipl.-Ing.
Graf, Christian, Ing.
Gratzer, Alexander J.
Grill, Claudia
Hasiba, Johann, Dipl.-Ing.
Hinterreiter, Jürgen, Dipl.-Ing.
Hofwimmer, Thomas, Ing.
Holmes, Justin C., Dr.
Höck, Eduard, Dipl.-Ing.
Hradecky, Doris
Hummel, Fabian N.J.
Jernej, Irmgard, Ing.
Jeszenszky, Harald, Dipl.-Ing.
Kargl, Günter, Dr.
Khodachenko, Maxim L., Dr.
Kiehas, Stefan, Dr.
Kirchner, Georg, Dr.
Koidl, Franz, Ing.
Korovinskiy, Daniil, Dr.
Kubyshkina, Daria, Dr.
Kürbisch, Christoph, Ing.
Laky, Gunter, Dipl.-Ing.
Lammer, Helmut, Doz.
Leichtfried, Mario, Ing.
Leitner, Stefan, Dipl.-Ing.
Lendl, Monika, Dr.
Lhotka, Christoph, Dr.
Lichtenegger, Herbert I.M., Dr.
Macher, Wolfgang, Dr.
Magnes, Werner, Dr.
Mannel, Thurid, MSc
Mautner, David
Möstl, Christian, Dr.
Muck, Cosima
Nakamura, Rumi, Doz.
Nakamura, Takuma K.M., Dr.
Narita, Yasuhito, Doz.
Neukirchner, Sonja, Ing.
Nischelwitzer-Fennes, Ute, Ing.
Ottacher, Harald, Dipl.-Ing.
Panov, Evgeny, Dr.
Pitterle, Martin
Plaschke, Ferdinand, Dr.
Pollinger, Andreas, Dr.
Posch, Oliver F.
Reiss, Martin A., Dr.
Roberts, Owen W., Dr.
Robinig, Lukas, BSc
Rojas-Castillo, Diana, Dr.
Sasunov, Yury, Dr.
Scherf, Manuel, Mag.
Scherr, Alexandra, Mag.
Schmid, Daniel, Dr.
Schweighart, Maria, BSc
Speckbacher, Lucas, BSc
Stachel, Manfred, Dipl.-Ing.
Steindorfer, Michael, Dr.
Steller, Manfred B., Dr.
Stieninger, Reinhard, Ing.
Sulis, Sophia, Dr.
Tiefenbacher, Patrick, Mag.
Tonfat Seclen, Jorge L., Dr.
Tschachler, Elvira, Mag.
Valavanoglou, Aris, Dipl.-Ing.
Varsani, Ali, Dr.
Voller, Wolfgang G., Mag.
Volwerk, Martin, Dr.
Vörös, Zoltan, Dr.
Wallner, Robert, Ing.
Wang, Peiyuan, Mag.
Wedlund, Cyril S., Dr.
Weiss, Andreas J., MSc
Wellenzohn, Simon, Dipl.-Ing.
Wilfinger, Josef, BSc
Young, Mitchell E., Dr.
Zhang, Tie-Long, Prof.

As of 31 December 2019

IMPRESSUM

PUBLISHER

Wolfgang Baumjohann, Director
Institut für Weltraumforschung (IWF)
Österreichische Akademie der Wissenschaften (ÖAW)
Schmiedlstraße 6, 8042 Graz, Austria
www.iwf.oeaw.ac.at

EDITORS

Bruno Besser, Alexandra Scherr, Martin Volwerk

DESIGN

Alexandra Scherr
pr.iwf@oeaw.ac.at
Twitter: @IWF_oeaw

PRINT

Servicebetrieb ÖH-Uni Graz GmbH


ÖAW IWF